AIMS Mathematics, 8(12): 28246–28279.
DOI: 10.3934/math.20231446
Received: 18 July 2023
Revised: 07 September 2023
Accepted: 28 September 2023
Published: 16 October 2023

http://www.aimspress.com/journal/Math

Research article

Novel codynamics of the HIV-1/HTLV-I model involving humoral immune response and cellular outbreak: A new approach to probability density functions and fractional operators

Hanan S. Gafel[1], **Saima Rashid**[2,3,*] **and Sayed K. Elagan**[1,4]

[1] Department of Mathematics and Statistics, College of Science, Taif University, P.O. Box 11099, Taif 21944, Saudi Arabia

[2] Department of Mathematics, Government College University, Faisalabad 38000, Pakistan

[3] Department of Natural Sciences, School of Arts and Sciences, Lebanese American University, Beirut 11022801, Lebanon

[4] Department of Mathematics and Computer Sciences, Faculty of Science Menoufia University, Shebin Elkom, Egypt

* **Correspondence:** Email: saimarashid@gcuf.edu.pk.

Abstract: Both human immunodeficiency virus type 1 (HIV-1) and human T-lymphotropic virus type I (HTLV-I) are retroviruses that afflict $CD4^+$ T cells. In this article, the codynamics of within-host HIV-1 and HTLV-I are presented via piecewise fractional differential equations by employing a stochastic system with an influential strategy for biological research. It is demonstrated that the scheme is mathematically and biologically feasible by illustrating that the framework has positive and bounded global findings. The necessary requirements are deduced, ensuring the virus's extinction. In addition, the structure is evaluated for the occurrence of an ergodic stationary distribution and sufficient requirements are developed. A deterministic-stochastic mechanism for simulation studies is constructed and executed in MATLAB to reveal the model's long-term behavior. Utilizing rigorous analysis, we predict that the aforesaid model is an improvement of the existing virus-to-cell and cell-to-cell interactions by investigating an assortment of behaviour patterns that include cross-over to unpredictability processes. Besides that, the piecewise differential formulations, which can be consolidated with integer-order, Caputo, Caputo-Fabrizio, Atangana-Baleanu and stochastic processes, have been declared to be exciting opportunities for researchers in a spectrum of disciplines by enabling them to incorporate distinctive features in various temporal intervals. As a result, by applying these formulations to difficult problems, researchers can achieve improved consequences in reporting realities with white noise. White noise in fractional HIV-1/HTLV-I codynamics plays an extremely important function in preventing the proliferation of an outbreak when the proposed flow is constant and disease extermination is directly proportional to the

magnitude of the white noise.

Keywords: HIV-1/HTLV-I codynamics model; fractional operators; deterministic-probabilistic models; extinction; ergodic and stationary distribution
Mathematics Subject Classification: 46S40, 47H10, 54H25

1. Introduction

Infectious diseases, also referred to as illnesses, have long been acknowledged as a constant danger to people worldwide. Contagious infections are those that can be transmitted from animals to humans, humans to humans or humans to animals. HIV-1 is a human pathogen that targets and infiltrates physically active $CD4^+$ T cells, which are essential constituents of the living person's immune response. Accumulated immunodeficiency virus (AIDS), a catastrophic autoimmune condition, plays a role in HIV-1. According to the World Health Organization (WHO), approximately 36.7 thousand individuals were thriving with HIV-1 at the end of 2017 and 2.0 million people were severely affected worldwide in 2016 [1]. In vitro tests show two ways HIV-1 spreads in vitro: virus-to-cell (VTC) and cell-to-cell (CTC). HIV-1 antimatter amassed by HIV-1-infected $CD4^+$ T cells seeks out additional better and healthier $CD4^+$ T mitochondria to infiltrate during VTC propagation. HIV-1 could be converted from immune-deficient CD^+T cells to stable CD^+T cells in the CTC phase of spread via immediate communication via antiviral therapy synaptic configuration. Numerous research findings have demonstrated that HIV-1 transmission via immediate CTC spread seems to be more productive and powerful than via VTC processing [2, 3]. According to Sigal et al. [4], HIV-1 CTC pervasiveness creates significant pathogens of balanced $CD4^+$T cells, reducing the effectiveness of therapeutic strategies. The immune system's two sets are cytotoxic T lymphocytes (CTLs) and autoantibodies for innate immunity. HIV-infected CD^+T cells are decapitated by CTLs, whereas HIV-1 granules are neutralized by B-cell immune cells.

HTLV-I causes diseases such as HTLV-I-associated myelopathy (HAM) and tropical spastic paraparesis (TSP). Between 11 and 21 million individuals globally are infected by HTLV-I. HTLV-I, such as HIV-1, infiltrates balanced $CD4^+$T cells. Precise CTC connection between HTLV-I-infected $CD4^+$T lymphocytes and balanced $CD4^+$T lymphocytes results in infestation [5]. The CTL inflammatory reaction is crucial for manipulating HTLV-I disease by solubilizing HTLV-I diseased $CD4^+$T cells [6]. Wu and Zhao [7] contemplated the dynamics of an HIV infection model with two infection routes and evolutionary competition between two viral strains. Wu et al. [8] expounded the evolution dynamics of a time-delayed reaction-diffusion HIV latent infection model with two strains and periodic therapies. Wu and Zhao [9] presented the dynamical analysis of a nonlocal delayed and diffusive HIV latent infection model with spatial heterogeneity.

Both HIV-1 and HTLV-I can indeed be carried from afflicted to un-immunized individuals via intimate intercourse, severely immuno-compromised items, intravenous fluids and stem cell therapy. HTLV-I may be injected through infant feed intake. Patients can be encountered all over the globe, including Germany, Asia, Brazil, Mexico, Tanzania and Portugal [10]. According to Isache et al. [11], the HTLV-I co-infection proportion among HIV-1-afflicted individuals is 95 to 600 times more than in

the general population. Co-dynamics with HTLV-I and HIV-1 may hasten the evolution of AIDS and pathogen improvement [12].

Mathematical modelling and simulation of viral illness can help with recognizing pathogen complexities within a host, evaluating various antiretroviral therapies and forecasting the evolution of sickness over time. Numerous investigators have worked to create and test numerical simulations of HIV-1 mono-infection, HTLV-I mono-infection and HIV-1/HTLV-I co-dynamics. Nowak et al. [13] established a predominant and benchmark HIV-1 mechanism framework that includes three divisions: Balanced $CD4^+$ T cells, effective HIV-1-infected $CD4^+$ T cells and unrestricted HIV-1 molecules. This analysis implies that HIV-1 inflammation is solely caused by V-T-C transmission. This framework has been customized to compensate for the two HIV-1 contagion mechanisms, VTC and CTC. Several studies have been inspired by the modelling of HIV-1 disease with VTC and CTC configurations of propagation and have specified supplemental biological pathways in the framework described in [14], such as: Lai and Zou [15] explored an HIV-1 infectious disease framework involving CTC transmission and different kinds of decentralized time delays, Wang et al. [16] incorporated latent diseased microbes and cytoplasmic delays into their framework of HIV-1 complexities for CTC propagation. Elaiw and Al-Shamrani [17] presented a comprehensive review of HIV-1 interactions in connection to the CTL immune system in contexts where CTC propagation is exacerbated by both deep-seated and productive virus particles. Ren et al. [18] investigated the consequences of CTC propagation, infection and cell flexibility on HIV-1 complexities. Wang et al. [19] investigated the maturity level of the HIV-1 approach that incorporates CTC spread. Al-Shamrani et al. [20] contemplated the HIV-1/HTLV-I infections framework incorporating innate immunity and a cellular pathogen.

Numerous quantitative ideas have been created throughout antiquity to aid us in comprehending the environment in which we reside. In regard to prediction, the notion of temporal and spatial modelling was implemented and advanced machine learning techniques were developed to control manifestations with moderate challenges. The notion of differentiation is one of the most frequently utilized computational theories in prognostication and modelling. This idea has been employed to create mathematical algorithms known as differential equations (DEs). The scientists proposed various formulae with complex correlations in the initial attempt, where differential formulations could be: local (exchange rate, conformable derivative and fractal derivative) [21–23]; not local with a singular kernel (Riemann-Liouville, Liouville-Caputo and various manifestations) [24]; local with a non-singular kernel (Caputo-Fabrizio operators) [25]; and eventually non-local and non-singular (Atangana-Baleanu operators) [26]. Several scholars recommend several groundbreaking orientations for the alternate meanings of differential derivatives or those who preplanned the underpinnings. Calculus with fractional order is affiliated with pragmatic endeavours and it is widely used in nanoscience, photonics, viral agents, quantum physics and image processing, among several other fields [21–23, 27].

Fractional calculus is a branch of numeracy and physical science that studies the behaviour of artefacts and technologies using fractional order differentiation. In contrast to integer-order configurations, fractional order simulations can encapsulate non-local spatial-temporal connections using recollection kernels of the index, exponential or Mittag-Leffler form law. The potential strengths of applying the fractional formulation of Atangana-Baleanu include every non-locality, which is intrinsic in its description, as is the case with all past iterations; even so, the key important

feature is that it possesses a nonsingular and non-local kernel, symbolized by the feature of Mittag-Leffler, that, from a quantitative perspective, encompasses the explanatory progression of capabilities demarcated by a sequence of prerogatives. Kumar and Kumar [28] presented a study on an eco-epidemiological model with fractional operators. Ghanbari et al. [29] investigated a behaviour for immune and tumor cells an immunogenetic tumour model with non-singular fractional derivative. However, the aforesaid formulation has been demonstrated to accurately represent the intricate patterns of assorted real-world manifestations [23, 27]. Unlike each derivative, Atangana and Araz [30] introduced the concept of the piecewise derivative, that can replicate the overlapping pathways of these fractional formulas in a differentiated methodology and has lately acquired popularity [31]. All of this suggests that the notified experiments are premised on a deterministic technique, whereas the existence of HIV-1/HTLV-I is stochastic rather than deterministic. Several scholars utilized the core idea of stochastic modelling to examine the evolution of communicable diseases in real life, as detailed in [32–34]. Because there is no latent infection in the stochastic structure, the virus's perseverance cannot be determined. Inevitably, the stationary distribution of the stochastic mechanism must be studied.

Based on the stochastic linear perturbation approach, in which the environmental white noise is proportional to the size of each subpopulation, a few stochastic HIV-1/HTLV-I models involving humoral immune response and cellular outbreak models have been established to analyze the impact of stochastic white noise and provide some effective measures to regulate disease dynamics. A stochastic HIV-1/HTLV-I model with a half-saturated incidence rate has been theoretically proven to suppress an HIV-1/HTLV-I outbreak. Inspired by such results [35–37], we similarly assume that the white noise is directly proportional to subpopulations $\mathcal{V}$, $\mathcal{G}^L$, $\mathcal{G}^A$, $\mathcal{U}^L$, $\mathcal{U}^A$, $\mathcal{T}$ and $\mathcal{Q}$. As a result, in this document, we attempted to demonstrate the noticeable impact of a stochastic scheme criterion stated in [20]. Furthermore, we develop a stochastic conceptual framework that analyses the HIV-1/HTLV-1 involving humoral immune response and cellular outbreak workflow in specified time intervals using piecewise fractional derivative formulations. To accomplish this, we divide the entire community into prevalence and distribution of the latent HIV-1-infected CD4$^+$ T cells and latent HTLV-I-infected CD4$^+$ T cells, as well as random fluctuations. The fraction coefficient $\lambda \in (0, 1)$ represents the likelihood that the latest HIV-1-infected CD4$^+$ T cells would be involved, while the surviving portion $1 - \lambda$ will be latent. We specifically demonstrated the existence and uniqueness of the codynamics of HIV-1/HTLV-I non-negative successful approach to exemplify that the framework is both quantitatively and biologically viable. We then investigate the extinction, ergodic and stationary distribution processes to determine the prerequisites for disease extinction and persistence. In a nutshell, numerical simulations of the projected model are investigated in fractional calculus theory, incorporating white noise and crossover patterns.

2. Model formulation and preliminaries

Al-Shamrani et al. [20] developed a codynamics of HIV-1/HTLV-I model in which humoral immunity and cellular infection coexist. The DEs depict the dynamical transmission of HIV-1/HTLV-I and the framework is as shown in:

$$\begin{cases} \frac{d\mathcal{V}}{d\mathbf{t}} = \vartheta - \beta\mathcal{V} - \upsilon_1\mathcal{V}\mathcal{T} - \upsilon_2\mathcal{V}\mathcal{G}^A - \upsilon_3\mathcal{V}\mathcal{U}^A \\ \frac{d\mathcal{G}^L}{d\mathbf{t}} = (1-\lambda)(\upsilon_1\mathcal{V}\mathcal{T} + \upsilon_2\mathcal{V}\mathcal{G}^A) - (\epsilon+\xi)\mathcal{G}^L \\ \frac{d\mathcal{G}^L}{d\mathbf{t}} = \lambda(\upsilon_1\mathcal{V}\mathcal{T} + \upsilon_2\mathcal{V}\mathcal{G}^A) + \epsilon\mathcal{G}^L - \varrho\mathcal{G}^A \\ \frac{d\mathcal{U}^L}{d\mathbf{t}} = \tau\upsilon_3\mathcal{V}\mathcal{U}^A - (\sigma+\varsigma)\mathcal{U}^L \\ \frac{d\mathcal{U}^A}{d\mathbf{t}} = \sigma\mathcal{U}^L - \phi\mathcal{U}^A \\ \frac{d\mathcal{T}}{d\mathbf{t}} = \omega_1\mathcal{G}^A - \rho\mathcal{T} - \omega_2\mathcal{Q}\mathcal{T} \\ \frac{d\mathcal{Q}}{d\mathbf{t}} = \delta\mathcal{Q}\mathcal{T} - \varkappa\mathcal{Q} \end{cases} \tag{2.1}$$

supplemented with initial conditions (ICs) $\mathcal{V}(0) \geq 0$, $\mathcal{G}^L \geq 0$, $\mathcal{G}^A \geq 0$, $\mathcal{U}^L \geq 0$, $\mathcal{U}^A \geq 0$, $\mathcal{T} \geq 0$, $\mathcal{Q} \geq 0$.

If $\mathbb{R}_0 < 1$, model (2.1) has a disease-free equilibrium which is globally asymptotically stable, given by $\mathcal{E}_0 = (\mathcal{H}_0, 0, 0, 0, 0, 0, 0) = (\frac{\vartheta}{\beta}, 0, 0, 0, 0, 0, 0)$. This new equilibrium identifies a health status in which both HIV-1 and HTLV-I are eliminated from the organ.

The system's (2.1) fundamental reproduction number is specified by

$$\mathbb{R}_0 = \frac{\vartheta(\omega_1\upsilon_1 + \rho\upsilon_2)(\epsilon + \lambda\xi)}{\beta\rho\varrho(\xi+\epsilon)}. \tag{2.2}$$

If $\mathbb{R}_0 > 1$, then model (2.1) satisfies an endemic equilibrium $\mathcal{E}^* = (\mathcal{V}^*, \mathcal{G}^{L*}, \mathcal{G}^{A*}, \mathcal{U}^{L*}, \mathcal{U}^{A*}, \mathcal{T}, \mathcal{Q})$ and the disease is uniformly persistent. Based on biological interpretations, all variables and factors are tabulated in Table 1.

2.1. Stochastic model

By taking into consideration the impact of white noise, we use the technique of Imhof et al. [49]. Assume that the structure's elements are inversely related to the random noise (2.1). The stochastic framework of strategy (2.1) then comes, as shown below:

$$\begin{cases} d\mathcal{V} = [\vartheta - \beta\mathcal{V} - \upsilon_1\mathcal{V}\mathcal{T} - \upsilon_2\mathcal{V}\mathcal{G}^A - \upsilon_3\mathcal{V}\mathcal{U}^A]d\mathbf{t} + \wp_1\mathcal{V}d\mathcal{Q}_1(\mathbf{t}), \\ d\mathcal{G}^L = [(1-\lambda)(\upsilon_1\mathcal{V}\mathcal{T} + \upsilon_2\mathcal{V}\mathcal{G}^A) - (\epsilon+\xi)\mathcal{G}^L]d\mathbf{t} + \wp_2\mathcal{G}^L d\mathcal{Q}_2(\mathbf{t}), \\ d\mathcal{G}^A = [\lambda(\upsilon_1\mathcal{V}\mathcal{T} + \upsilon_2\mathcal{V}\mathcal{G}^A) + \epsilon\mathcal{G}^L - \varrho\mathcal{G}^A]d\mathbf{t} + \wp_3\mathcal{G}^A d\mathcal{Q}_3(\mathbf{t}), \\ d\mathcal{U}^L = [\tau\upsilon_3\mathcal{V}\mathcal{U}^A - (\sigma+\varsigma)\mathcal{U}^L]d\mathbf{t} + \wp_4\mathcal{U}^L d\mathcal{Q}_4(\mathbf{t}), \\ d\mathcal{U}^A = [\sigma\mathcal{U}^L - \phi\mathcal{U}^A]d\mathbf{t} + \wp_5\mathcal{U}^A d\mathcal{Q}_5(\mathbf{t}), \\ d\mathcal{T} = [\omega_1\mathcal{G}^A - \rho\mathcal{T} - \omega_2\mathcal{Q}\mathcal{T}]d\mathbf{t} + \wp_6\mathcal{T}d\mathcal{Q}_6(\mathbf{t}), \\ d\mathcal{Q} = [\delta\mathcal{Q}\mathcal{T} - \varkappa\mathcal{Q}]d\mathbf{t} + \wp_7\mathcal{Q}d\mathcal{Q}_7(\mathbf{t}), \end{cases} \tag{2.3}$$

where $\mathcal{Q}_\iota(\mathbf{t})$, $\iota = 1, ..., 7$ are independent standard Brownian motions having $\mathcal{Q}_\iota(0) = 0$ and $\wp_\iota^2 > 0$ are instances of white noise for $\iota = 1, ..., 7$. The initial conditions (ICs) have been the same as in the framework (2.3).

Table 1. Explanation of the biological scaling variables in the system (2.1).

Symbols	Explanation	Value	References
$\mathcal{V}$	Wellbeing CD4$^+$ T cells		
$\mathcal{G}^L$	CD4$^+$ T cells afflicted with HIV-1 that are latent		
$\mathcal{G}^A$	Effective HIV-1-afflicted CD4$^+$ T cells		
$\mathcal{U}^L$	CD4$^+$ T cells afflicted with HTLV-I that are latent		
$\mathcal{U}^A$	Effective HTLV-I-afflicted CD4$^+$ T cells		
$\mathcal{T}$	HIV-1 particles		
$\mathcal{Q}$	HIV-1 Restricted antibodies		
ϑ	Availability of balanced CD4$^+$ T cells	10	[34, 38]
β	Mortality risk of balanced CD4$^+$ T cells	0.01	[39, 40]
υ_1	Rate of pathogenic virus caused by interaction between HIV-1 granules and balanced CD4$^+$ T cells	varied	-
υ_2	Rate of cellular infestation caused by interaction between effective immunodeficient cells and balanced CD4$^+$ T cells	varied	-
υ_3	Rate of cellular infestation resulted from interaction between effective HTLV-I-infected cells and balanced CD4$^+$ T cells	varied	-
$\lambda \in (0, 1)$	Proportion coefficient denotes the likelihood of fresh HIV-1-infected cells becoming operative and the residual portion 1 will be passive	0.3	[41]
ϵ	Rates of stimulation of innate HIV-1-infected CD4$^+$ T cells	0.4	Supposed
ξ	Mortality risk of CD4$^+$ T cells contaminated with innate HIV-1	0.1	[41]
ϱ	Mortality risk of CD4$^+$ T cells contaminated with energetic HIV-1	0.5	[42–44]
$\tau \in (0, 1)$	Possibility of fresh HTLV-I pathogens entering an unexpressed duration	0.2	[45]
σ	Rates of stimulation of hidden HTLV-I-pathogenic CD4$^+$ T cells	0.5	Supposed
ϖ	Mortality risk of hidden HTLV-I-pathogenic CD4$^+$ T cells	0.3	Supposed
φ	Mortality risk of energetic HTLV-I-pathogenic CD4$^+$ T cells	0.2	[46, 47]
ω_1	Generation of unrestricted HIV-1 granules	5	[34]
ρ	Mortality risk of HIV-1 particles	2	[34]
ω_2	Inactivation rate of HIV-1 particulate by HIV-1-particular antibody levels	0.8	Supposed
δ	HIV-1-specific antibody prevalence	varied	-
$\varkappa$	Mortality risk of HIV-1-particular antibodies	0.1	[48]

For the sake of straightforwardness, assume an exhaustive probability space $(\aleph, \mathfrak{F}, \{\mathfrak{F}_\mathbf{t}\}_{\mathbf{t}\geq 0}, \mathbb{P})$ containing filtration $\{\mathfrak{F}_\mathbf{t}\}_{\mathbf{t}\geq 0}$ maintaining regular suppositions in mind (i.e., increasing and right continuous for $\mathfrak{F}_0$ contains every $\mathcal{T}$-null sets) and $\mathcal{Q}_\iota(\mathbf{t})$, $\iota = 1, ..., 8$ are stated in $(\aleph, \mathfrak{F}, \{\mathfrak{F}_\mathbf{t}\}_{\mathbf{t}\geq 0}, \mathbb{P})$. Also, consider $\mathbb{R}_+ = \{\mathbf{y} \geq 0\}$, $\mathbb{R}_+^7 = \{\bar{\mathbf{y}} = (\mathbf{y_1}, ..., \mathbf{y}_7) \in \mathbb{R}^7 : \mathbf{y}_\iota > 0,\ \iota = 1, ..., 8\}$. Let us suppose $\mathbf{M}^T$ is the transpose of $\mathbf{M}$. Symbolize $\bar{\mathbf{y}}(\mathbf{t}) = (\mathcal{V}(\mathbf{t}), \mathcal{G}^L(\mathbf{t}), \mathcal{G}^A(\mathbf{t}), \mathcal{U}^L(\mathbf{t}), \mathcal{U}^A(\mathbf{t}), \mathcal{T}(\mathbf{t}), \mathcal{Q}(\mathbf{t}))^T$ as the main finding of (2.3) supplemented by ICs $\bar{\mathbf{y}}(0) = (\mathcal{V}(0), \mathcal{G}^L(0), \mathcal{G}^A(0), \mathcal{U}^L(0), \mathcal{U}^A(0), \mathcal{T}(0), \mathcal{Q}(0))^T$. Moreover, take $z_1 \vee z_2 = \max\{z_1, z_2\}$ and $z_1 \wedge z_2 = \min\{z_1, z_2\}$.

The stochastic DE in $\tilde{d}$-dimensions is outlined as:

$$d\mathbf{w}(\mathbf{t}) = \Theta_1(\mathbf{w}(\mathbf{t}), \mathbf{t})d\mathbf{t} + \Theta_2(\mathbf{w}(\mathbf{t}), \mathbf{t})dB(\mathbf{t}),\ \mathbf{w}(\mathbf{t}_0) = \mathbf{w}_0,\ \forall\ \mathbf{t}_0 \leq \mathbf{t} \leq \mathsf{T} < \infty, \tag{2.4}$$

where $\Theta_1 : \mathbb{R}^{\tilde{d}} \times [\mathbf{t}_0, \mathsf{T}] \mapsto \mathbb{R}^{\tilde{d}}$ and $\Theta_2 : \mathbb{R}^{\tilde{d}} \times [\mathbf{t}_0, \mathsf{T}] \mapsto \mathbb{R}^{\tilde{d}\times m_1}$ are Borel measurable containing $\mathbf{B} = \{\mathbf{B}(\mathbf{t})\}_{\mathbf{t}\geq\mathbf{t}_0}$ is an $\mathbb{R}^{m_1}$-valued Wiener approach and $\mathbf{w}_0$ is an $\mathbb{R}^{\tilde{d}}$-valued r.v defined on F.

Furthermore, $\mathbb{C}^{2,1}(\mathbb{R}^{\tilde{d}} \times [\mathbf{t}_0, \infty); \mathbb{R}_+)$ is considered as the set of all non-negative functions $\mathbf{S}(\mathbf{w}, \mathbf{t})$ on $\mathbb{R}^{\tilde{d}} \times [\mathbf{t}_0, \infty)$ that are continuously twice differentiable in $\mathbf{w} \in \mathbb{R}^{\tilde{d}}$ and once in $\mathbf{t} \in [\mathbf{t}_0, \infty)$. The differential function $\mathbb{L}$ for the stochastic DE (2.4) is outlined as:

$$\mathbb{L} = \frac{\partial}{\partial \mathbf{t}} + \sum_{\mathbf{p}=1}^{\tilde{d}} \Theta_{1\mathbf{p}}(\mathbf{w}, \mathbf{t}) \frac{\partial}{\partial \mathbf{w}_\mathbf{p}} + \frac{1}{2} \sum_{\mathbf{i},\mathbf{p}=1}^{\tilde{d}} \sum_{J=1}^{m_1} \Theta_{2\mathbf{p}_J}(\mathbf{w}, \mathbf{t}) \Theta_{2\mathbf{p}_J}(\mathbf{w}, \mathbf{t}) \frac{\partial^2}{\partial \mathbf{w}_\mathbf{p} \partial \mathbf{w}_\mathbf{i}}.$$

Introduce the function $\mathbf{H} \in \mathbb{C}^{2,1}(\mathbb{R}^{\tilde{d}} \times [\mathbf{t}_0, \infty)$, then

$$\mathbb{L}\mathbf{H}(\mathbf{w}, \mathbf{t}) = \mathbf{H}_\mathbf{t}(\mathbf{w}, \mathbf{t}) + \mathbf{H}_\mathbf{w}(\mathbf{w}, \mathbf{t})\Theta_1(\mathbf{w}, \mathbf{t}) + \frac{1}{2} \sum_{\mathbf{i},\mathbf{p}=1}^{\tilde{d}} \sum_{J=1}^{m_1} \Theta_{2\mathbf{i}_J}(\mathbf{w}, \mathbf{t}) \Theta_{2\mathbf{p}_J}(\mathbf{w}, \mathbf{t}) \mathbf{H}_{\mathbf{ww}}(\mathbf{w}, \mathbf{t}),$$

where $\mathbf{H}_\mathbf{t} := \frac{\partial \mathbf{H}}{\partial \mathbf{t}}$; $\mathbf{H}_{\mathbf{s}_1} = (\mathbf{H}_{\mathbf{w}_\mathbf{p}}, ..., \mathbf{H}_{\mathbf{w}_{\tilde{d}}})$, $\mathbf{H}_{\mathbf{ww}} = (\mathbf{H}_{\mathbf{w}_\mathbf{p}}, \mathbf{H}_{\mathbf{w}_\mathbf{p}})_{\tilde{d}\times\tilde{d}}$.

For $\mathbf{w}(\mathbf{t}) \in \mathbb{R}^{\tilde{d}}$, then Itô's formula is presented as:

$$d\mathbf{H}(\mathbf{w}(\mathbf{t}), \mathbf{t}) = \mathbb{L}\mathbf{H}(\mathbf{w}(\mathbf{t}), \mathbf{t})d\mathbf{t} + \mathbf{H}_\mathbf{w}(\mathbf{w}(\mathbf{t}), \mathbf{t})\Theta_2(\mathbf{w}(\mathbf{t}), \mathbf{t})d\mathcal{Q}(\mathbf{t}).$$

We offer the corresponding overview below to assist individuals in becoming familiar with fractional calculus [24–26].

$${}_0^C\mathbf{D}_\mathbf{t}^\eta \mathbf{F}(\mathbf{t}) = \frac{1}{\Gamma(1-\eta)} \int_0^\mathbf{t} \mathbf{F}'(\mathbf{w})(\mathbf{t}-\mathbf{w})^\eta d\mathbf{w}, \quad \eta \in (0, 1].$$

$${}_0^{CF}\mathbf{D}_\mathbf{t}^\eta \mathbf{F}(\mathbf{t}) = \frac{\mathbf{Z}(\eta)}{1-\eta} \int_0^\mathbf{t} \mathbf{F}'(\mathbf{w}) \exp\Big[-\frac{\eta}{1-\eta}(\mathbf{t}-\mathbf{w})\Big] d\mathbf{w}, \quad \eta \in (0, 1],$$

where $\mathbf{Z}(\eta)$ is considered to be normalized mapping with $\mathbf{Z}(0) = \mathbf{Z}(1) = 1$.

The following is the structure of the Atangana-Baleanu derivative:

$${}_0^{ABC}\mathbf{D}_\mathbf{t}^\eta \mathbf{F}(\mathbf{t}) = \frac{ABC(\eta)}{1-\eta} \int_0^\mathbf{t} \mathbf{F}'(\mathbf{w}) E_\eta\Big[-\frac{\eta}{1-\eta}(\mathbf{t}-\mathbf{w})^\eta\Big] d\mathbf{w}, \quad \eta \in (0, 1],$$

where $ABC(\eta) = 1 - \eta + \frac{\eta}{\Gamma(\eta)}$ signifies the normalization function.

2.2. Existence-uniqueness of positive solutions

The accompanying consequence is suggested to define the (2.3) existence-uniqueness of the stochastic approach.

Theorem 2.1. *Assume that the stochastic system* (2.3) *for* $\mathbf{t} \geq 0$ *containing ICs* $\tilde{\mho}(0) \in \mathbb{R}_+^7$ *has a unique solution. Furthermore, the solution of* $\tilde{\mho}(\mathbf{t})$ *occurs in* $\mathbb{R}_+^7$ *almost surely (1.e)* 1, *i.e.,* $\tilde{\mho}(0) \in \mathbb{R}_+^7 \ \ \forall\ \mathbf{t} \geq 0$.

Proof. Consider the model parameters $\tilde{\mho}(\mathbf{t}) \in \mathbb{R}_+^7$ are continuous and locally lipschtz supplemented with ICs. Consequently, the model $\tilde{\mho}(\mathbf{t})$ has a unique solution for $\mathbf{t} \in [0, \ell_\varepsilon)$. The explosive period ℓ_ε is completely investigated in [50]. To demonstrate the solution's versatility, we have to illustrate that $\ell_\varepsilon = \infty$ (a.s). Consider we hold a sufficiently large positive number χ_0 such that the ICs of all conditions come up within the specified time frame $[\chi_0, \frac{1}{\chi_0}]$. Selecting $\chi \geq \chi_0$ be the final time requirements for every positive integer,

$$\ell_\chi = \inf\Big\{\mathbf{t} \in [0, \ell_\varepsilon) : \min\{\tilde{\mho}(\mathbf{t})\} \leq \frac{1}{\chi} \; or \; \max\{\tilde{\mho}(\mathbf{t})\} \geq \chi\Big\}.$$

During this research process, we utilize $\inf \emptyset = \infty$, whereas $\emptyset$ presents a null set. This technique χ encourages us to assert that this figure expands as χ tends to ∞. Taking $\ell_\infty = \lim_{\chi \mapsto \infty} \ell_\varepsilon \geq \ell_\infty$ (a.s). Following affirming that $\ell_\infty = \infty$ (a.s), We'll challenge the argument that $\ell_\varepsilon = \infty$ and thus $\tilde{\mho}(\mathbf{t})$ occur in $\mathbb{R}_+^7$ a.s $\forall\, \mathbf{t} \geq 0$. So, verifying that $\ell_\infty = \infty$ (a.s). We assume two positive determined numbers for the above $\varepsilon \in (0, 1)$ and T must exist such that

$$P\{\mathsf{T} \geq \ell_\infty\} > \epsilon. \tag{2.5}$$

Therefore, the integer $\upsilon_1 \geq \chi_0$ occurs in the following form

$$P\{\mathsf{T} \geq \ell_\chi\} \geq \epsilon, \; \upsilon_1 \leq \chi.$$

Thus, we aim to present a function $\mathcal{J} : \mathbb{R}_+^7 \mapsto \mathbb{R}_+$ in this form:

$$\mathcal{J}(\tilde{\mho}(\mathbf{t})) = \mathcal{V} + \mathcal{G}^L + \mathcal{G}^A + \mathcal{U}^L + \mathcal{U}^A + \mathcal{T} + \mathcal{Q} - 7 - (\mathcal{V} + \mathcal{G}^L + \mathcal{G}^A + \mathcal{U}^L + \mathcal{U}^A + \mathcal{T} + \mathcal{Q}). \tag{2.6}$$

In accordance with the criteria, $0 \leq \mathbf{w}_1 - \ln \mathbf{w}_1 - 1, \; \forall \mathbf{w}_1 > 0$, we find $\mathcal{J}(\tilde{\mho}(\mathbf{t}))$ is a positive mapping. Assume the random terminology $\chi_0 \leq \chi$ and $\mathsf{T} > 0$.
Considering Ito's approach to (2.6) produces

$$\begin{aligned} d\mathcal{J}(\tilde{\mho}(\mathbf{t})) \quad &= \mathbf{L}\mathcal{J}(\tilde{\mho}) + \wp_1(\mathcal{V} - 1)d\mathcal{Q}_1(\mathbf{t}) + \wp_2(\mathcal{G}^L - 1)d\mathcal{Q}_2(\mathbf{t}) + \wp_3(\mathcal{G}^A - 1)d\mathcal{Q}_3(\mathbf{t}) \\ &\quad + \wp_4(\mathcal{U}^L - 1)d\mathcal{Q}_4(\mathbf{t}) + \wp_5(\mathcal{U}^A - 1)d\mathcal{Q}_5(\mathbf{t}) + \wp_6(\mathcal{T} - 1)d\mathcal{Q}_6(\mathbf{t}) + \wp_7(\mathcal{Q} - 1)d\mathcal{Q}_7(\mathbf{t}). \end{aligned} \tag{2.7}$$

Considering (2.8), define the following functional $\mathbf{L}\mathcal{J} : \mathbb{R}_+^7 \mapsto \mathbb{R}_+$ as:

$$\begin{aligned} \mathbf{L}\mathcal{J} \quad &= \Big(1 - \frac{1}{\mathcal{V}}\Big)\Big(\vartheta - \beta\mathcal{V} - \upsilon_1\mathcal{V}\mathcal{T} - \upsilon_2\mathcal{V}\mathcal{G}^A - \upsilon_3\mathcal{V}\mathcal{U}^A\Big) + \frac{\wp_1^2}{2} \\ &\quad + \Big(1 - \frac{1}{\mathcal{G}^L}\Big)\Big((1 - \lambda)(\upsilon_1\mathcal{V}\mathcal{T} + \upsilon_2\mathcal{V}\mathcal{G}^A) - (\epsilon + \xi)\mathcal{G}^L\Big) + \frac{\wp_2^2}{2} \\ &\quad + \Big(1 - \frac{1}{\mathcal{G}^A}\Big)\Big(\lambda(\upsilon_1\mathcal{V}\mathcal{T} + \upsilon_2\mathcal{V}\mathcal{G}^A) + \epsilon\mathcal{G}^L - \varrho\mathcal{G}^A\Big) + \frac{\wp_3^2}{2} \\ &\quad + \Big(1 - \frac{1}{\mathcal{U}^L}\Big)\Big(\tau\upsilon_3\mathcal{V}\mathcal{U}^A - (\sigma + \varsigma)\mathcal{U}^L\Big) + \frac{\wp_4^2}{2} \\ &\quad + \Big(1 - \frac{1}{\mathcal{U}^A}\Big)\Big(\sigma\mathcal{U}^L - \phi\mathcal{U}^A\Big) + \frac{\wp_5^2}{2} \end{aligned}$$

$$
\begin{aligned}
&+\Big(1-\frac{1}{\mathcal{T}}\Big)\Big(\omega_1\mathcal{G}^A-\rho\mathcal{T}-\omega_2\mathcal{Q}\mathcal{T}\Big)+\frac{\wp_6^2}{2}\\
&+\Big(1-\frac{1}{\mathcal{Q}}\Big)\Big(\delta\mathcal{Q}\mathcal{T}-\varkappa\mathcal{Q}\Big)+\frac{\wp_7^2}{2}\\
&=\vartheta+\beta+(\epsilon+\xi)+\varrho+(\sigma+\varsigma)+\phi+\rho+\varkappa-\beta\mathcal{V}-\upsilon_1\mathcal{V}\mathcal{T}-\upsilon_2\mathcal{V}\mathcal{G}^A-\upsilon_3\mathcal{V}\mathcal{U}^A\\
&\quad+(1-\lambda)(\upsilon_1\mathcal{V}\mathcal{T}+\upsilon_2\mathcal{V}\mathcal{G}^A)-(\epsilon+\xi)\mathcal{G}^L+\lambda(\upsilon_1\mathcal{V}\mathcal{T}+\upsilon_2\mathcal{V}\mathcal{G}^A)+\epsilon\mathcal{G}^L-\varrho\mathcal{G}^A+\sigma\mathcal{U}^L-\phi\mathcal{U}^A\\
&\quad+\omega_1\mathcal{G}^A-\rho\mathcal{T}-\omega_2\mathcal{Q}\mathcal{T}+\delta\mathcal{Q}\mathcal{T}-\varkappa\mathcal{Q}+\frac{\wp_1^2+\wp_2^2+\wp_3^2+\wp_4^2+\wp_5^2+\wp_6^2+\wp_7^2}{2}\\
&\leq\vartheta+\beta+(\epsilon+\xi)+\varrho+(\sigma+\varsigma)+\phi+\rho+\varkappa+\frac{\wp_1^2+\wp_2^2+\wp_3^2+\wp_4^2+\wp_5^2+\wp_6^2+\wp_7^2}{2}:=\Omega.
\end{aligned}
$$

For a positive constant ς, it is independent of $\tilde{\mho}$ as well as of $\mathbf{t}$. So, we get

$$
\begin{aligned}
d\mathcal{J}(\tilde{\mho}) \quad &=\Omega d\mathbf{t}+\wp_1(\mathcal{V}-1)d\mathcal{Q}_1(\mathbf{t})+\wp_2(\mathcal{G}^L-1)d\mathcal{Q}_2(\mathbf{t})+\wp_3(\mathcal{G}^A-1)d\mathcal{Q}_3(\mathbf{t})\\
&\quad+\wp_4(\mathcal{U}^L-1)d\mathcal{Q}_4(\mathbf{t})+\wp_5(\mathcal{U}^A-1)d\mathcal{Q}_5(\mathbf{t})+\wp_6(\mathcal{T}-1)d\mathcal{Q}_6(\mathbf{t})\\
&\quad+\wp_7(\mathcal{Q}-1)d\mathcal{Q}_7(\mathbf{t}).
\end{aligned}\tag{2.8}
$$

Furthermore, we have

$$
\begin{aligned}
&\mathbf{E}\Big[\mathcal{J}(\mathcal{V}(\ell_\chi\wedge\mathsf{T}),\mathcal{G}^L(\ell_\chi\wedge\mathsf{T}),\mathcal{G}^A(\ell_\chi\wedge\mathsf{T}),\mathcal{U}^L(\ell_\chi\wedge\mathsf{T}),\mathcal{U}^A(\ell_\chi\wedge\mathsf{T}),\mathcal{T}(\ell_\chi\wedge\mathsf{T}),\mathcal{Q}(\ell_\chi\wedge\mathsf{T}))\Big]\\
&\leq\mathcal{J}(\tilde{\mho}(0))+\mathbf{E}\Big\{\int_0^{\ell_\chi\wedge\mathsf{T}}\Omega d\mathbf{t}\Big\}\\
&\leq\mathcal{J}(\tilde{\mho}(0))+\Omega\,\mathsf{T}\,.
\end{aligned}\tag{2.9}
$$

Choosing $\Psi_\chi=\{\ell_\chi\leq\mathsf{T}\}$ for $\chi\geq\upsilon_1$ and (2.5) produces that $P(\Psi_{\omega_1})\geq\epsilon$. Evidently, every ς from Ψ_χ has one or more $\mathcal{V}(\ell_\chi,\varsigma),\mathcal{G}^L(\ell_\chi,\varsigma),\mathcal{G}^A(\ell_\chi,\varsigma),\mathcal{U}^L(\ell_\chi,\varsigma),\mathcal{U}^A(\ell_\chi,\varsigma),\mathcal{T}(\ell_\chi,\varsigma)$ and $\mathcal{Q}(\ell_\chi,\varsigma)$ that are identical to $\frac{1}{\chi}$ or χ. Therefore, $\mathcal{J}(\mathcal{V}(\ell_\chi),\mathcal{G}^L(\ell_\chi),\mathcal{G}^A(\ell_\chi),\mathcal{U}^L(\ell_\chi),\mathcal{U}^A(\ell_\chi),\mathcal{T}(\ell_\chi),\mathcal{Q}(\ell_\chi))$ is no less than $\ln\chi-1+\frac{1}{\chi}$ or $\chi-1-\ln\chi$.
Finally,

$$
\mathcal{J}(\mathcal{V}(\ell_\chi),\mathcal{G}^L(\ell_\chi),\mathcal{G}^A(\ell_\chi),\mathcal{U}^L(\ell_\chi),\mathcal{U}^A(\ell_\chi),\mathcal{T}(\ell_\chi),\mathcal{Q}(\ell_\chi))\geq\Big(\ln\chi-1+\frac{1}{\chi}\Big)\wedge\mathbf{E}(\chi-1-\ln\chi).
$$

Making the use of (2.5) and (2.9), we have

$$
\begin{aligned}
\mathcal{J}(\tilde{\mho}(0))+\Omega_{\mathsf{T}} \quad &\geq\mathbf{E}\Big[1_{\Psi(\varsigma)}\mathcal{J}(\mathcal{V}(\ell_\chi),\mathcal{G}^L(\ell_\chi),\mathcal{G}^A(\ell_\chi),\mathcal{U}^L(\ell_\chi),\mathcal{U}^A(\ell_\chi),\mathcal{T}(\ell_\chi),\mathcal{Q}(\ell_\chi))\Big]\\
&\geq\epsilon\Big\{\Big(\ln\chi-1+\frac{1}{\chi}\Big)\wedge(\chi-1-\ln\chi)\Big\}.
\end{aligned}
$$

Observing that, the indicator function Ψ is $1_{\Psi(\varsigma)}$. Therefore, it tends to ∞ and produces the contradiction $\infty>\mathcal{J}(\tilde{\mho}(0))+\Omega_{\mathsf{T}}=\infty$, indicating that $\ell_\infty=\infty$ a.s.

2.3. The elimination of HIV-1/HTLV-I infection

In what follows, we intend to calculate the significant value for disease eradication. We determine how to regulate the subtleties of the disease so that it eventually appears to become extinct over time, which is a significant factor in the transmission of infection.

This section examines at the framework's extinction and ergodic stationary distributions (ESD). Let us present

$$\langle \mathcal{G}^A(\mathbf{t})\rangle = \frac{1}{\mathbf{t}}\int_0^{\mathbf{t}} \mathbf{y}(\mathbf{s})d\mathbf{s}. \tag{2.10}$$

Following that, we will discuss the widely recognized consequence of the strong law of huge quantities, which is primarily attributed to [51].

Lemma 2.1. *([51]) Assume that a local martingale for continuous and real-valued mapping* $\mathbf{Z} = \{\mathbf{Z}\}_{\mathbf{t}\geq 0}$ *goes extinct as* $\mathbf{t} \mapsto 0$, *then*

$$\lim_{\mathbf{t}\mapsto\infty}\langle \mathbf{Z},\mathbf{Z}\rangle_{\mathbf{t}} = \infty,\ a.s.,\ \Longrightarrow\ \lim_{\mathbf{t}\mapsto\infty}\frac{\mathbf{Z}_{\mathbf{t}}}{\langle \mathbf{Z},\mathbf{Z}\rangle_{\mathbf{t}}} = 0,\ a.s.,\ and\ also$$

$$\lim_{\mathbf{t}\mapsto\infty}\frac{\langle \mathbf{Z},\mathbf{Z}\rangle_{\mathbf{t}}}{\mathbf{t}} < 0,\ a.s.,\ \Longrightarrow\ \lim_{\mathbf{t}\mapsto\infty}\frac{\mathbf{Z}_{\mathbf{t}}}{\mathbf{t}} = 0,\ a.s.$$

Let us categorize an additional threshold value for our future necessities:

$$\mathbb{R}_0^p = \frac{\vartheta\lambda\upsilon_2}{\beta(\varrho + \frac{\wp_3^2}{2})}. \tag{2.11}$$

Theorem 2.2. *For* $\tau > \frac{1}{2}(\wp_1^2 \vee \wp_2^2 \vee \wp_3^2 \vee \wp_4^2 \vee \wp_5^2 \vee \wp_6^2 \vee \wp_7^2)$ *and surmise that for positive solution* $\tilde{\mho}(\mathbf{t})$ *for the system* (2.3) *supplemented with ICs* $\tilde{\mho}(0) \in \mathbb{R}_+^7$, *we obtain:*

If $\mathbb{R}_0^p < 1$, *then*

$$\limsup_{\mathbf{t}\mapsto\infty}\frac{\ln \mathcal{G}^A(\mathbf{t})}{\mathbf{t}} \leq \Big(\varrho + \frac{\wp_3^2}{2}\Big)\Big\{\mathbb{R}_0^p - 1\Big\} < 0\ a.s.,$$

which suggests that the infection will be eradicated in future generations. Also,

$$\lim_{\mathbf{t}\mapsto\infty}\mathcal{V}(\mathbf{t}) = \frac{\vartheta}{\beta},\ \lim_{\mathbf{t}\mapsto\infty}\mathcal{G}^L(\mathbf{t}) = 0,\ \lim_{\mathbf{t}\mapsto\infty}\mathcal{G}^A(\mathbf{t}) = 0,\ \lim_{\mathbf{t}\mapsto\infty}\mathcal{U}^L(\mathbf{t}) = \frac{\tau}{\vartheta+\lambda_3},\ \lim_{\mathbf{t}\mapsto\infty}\mathcal{U}^A(\mathbf{t}) = 0,$$
$$\lim_{\mathbf{t}\mapsto\infty}\mathcal{T}(\mathbf{t}) = 0,\ \lim_{\mathbf{t}\mapsto\infty}\mathcal{Q}(\mathbf{t}) = 0.$$

Proof. Employing integration on (2.3), we get

$$\frac{\mathcal{V}(\mathbf{t})-\mathcal{V}(0)}{\mathbf{t}} = \vartheta - \beta\langle\mathcal{V}(\mathbf{t})\rangle - \upsilon_1\langle\mathcal{V}(\mathbf{t})\mathcal{T}(\mathbf{t})\rangle - \upsilon_2\langle\mathcal{V}(\mathbf{t})\mathcal{G}^A(\mathbf{t})\rangle - \upsilon_3\langle\mathcal{V}(\mathbf{t})\mathcal{U}^A(\mathbf{t})\rangle + \frac{\wp_1}{\mathbf{t}}\int_0^{\mathbf{t}}\mathcal{V}(s_1)d\mathcal{Q}_1(s_1),$$

$$\frac{\mathcal{G}^L(\mathbf{t})-\mathcal{G}^L(0)}{\mathbf{t}} = (1-\lambda)(\upsilon_1\langle\mathcal{V}(\mathbf{t})\mathcal{T}(\mathbf{t})\rangle + \upsilon_2\langle\mathcal{V}(\mathbf{t})\mathcal{G}^A(\mathbf{t})\rangle) - (\epsilon+\xi)\langle\mathcal{G}^L(\mathbf{t})\rangle + \frac{\wp_2}{\mathbf{t}}\int_0^{\mathbf{t}}\mathcal{G}^L(s_1)d\mathcal{Q}_2(s_1),$$

$$\frac{\mathcal{G}^A(\mathbf{t})-\mathcal{G}^A(0)}{\mathbf{t}} = \lambda(\upsilon_1\langle\mathcal{V}(\mathbf{t})\mathcal{T}(\mathbf{t})\rangle + \upsilon_2\langle\mathcal{V}(\mathbf{t})\mathcal{G}^A(\mathbf{t})\rangle) + \epsilon\langle\mathcal{G}^L(\mathbf{t})\rangle - \varrho\langle\mathcal{G}^A(\mathbf{t})\rangle + \frac{\wp_3}{\mathbf{t}}\int_0^{\mathbf{t}}\mathcal{G}^A(s_1)d\mathcal{Q}_3(s_1),$$

$$\frac{\mathcal{U}^L(\mathbf{t})-\mathcal{U}^L(0)}{\mathbf{t}}=\tau\upsilon_3\langle\mathcal{V}(\mathbf{t})\mathcal{U}^A(\mathbf{t})\rangle-(\sigma+\varsigma)\langle\mathcal{U}^L(\mathbf{t})\rangle+\frac{\wp_4}{\mathbf{t}}\int_0^{\mathbf{t}}\mathcal{U}^L(s_1)d\mathcal{Q}_4(s_1),$$

$$\frac{\mathcal{U}^A(\mathbf{t})-\mathcal{U}^A(0)}{\mathbf{t}}=\sigma\langle\mathcal{U}^L(\mathbf{t})\rangle-\phi\langle\mathcal{U}^A(\mathbf{t})\rangle+\frac{\wp_5}{\mathbf{t}}\int_0^{\mathbf{t}}\mathcal{G}^A(s_1)d\mathcal{Q}_5(s_1),$$

$$\frac{\mathcal{T}(\mathbf{t})-\mathcal{T}(0)}{\mathbf{t}}=\omega_1\langle\mathcal{G}^A(\mathbf{t})\rangle-\rho\langle\mathcal{T}(\mathbf{t})\rangle-\omega_2\langle\mathcal{Q}(\mathbf{t})\mathcal{T}(\mathbf{t})\rangle+\frac{\wp_6}{\mathbf{t}}\int_0^{\mathbf{t}}\mathcal{T}(s_1)d\mathcal{Q}_6(s_1),$$

$$\frac{\mathcal{Q}(\mathbf{t})-\mathcal{Q}(0)}{\mathbf{t}}=\delta\langle\mathcal{Q}(\mathbf{t})\mathcal{T}(\mathbf{t})\rangle-\varkappa\langle\mathcal{Q}(\mathbf{t})\rangle+\frac{\wp_7}{\mathbf{t}}\int_0^{\mathbf{t}}\mathcal{Q}(s_1)d\mathcal{Q}_7(s_1). \tag{2.12}$$

Considering Itô's technique on $\ln(\mathcal{G}^A(\mathbf{t}))$, we attain

$$\ln(\mathcal{G}^A(\mathbf{t}))=\Big\{\lambda\Big(\upsilon_1\frac{\mathcal{V}\mathcal{T}}{\mathcal{G}^A}+\upsilon_2\mathcal{V}\Big)+\epsilon\frac{\mathcal{G}^L}{\mathcal{G}^A}-\Big(\varrho+\frac{\wp_3}{2}\Big)\Big\}d\mathbf{t}+\wp_3 d\mathcal{Q}_3(\mathbf{t}).$$

Performing integration over $(0,\mathbf{t})$, we get

$$\ln(\mathcal{G}^A(\mathbf{t}))-\ln(\mathcal{G}^A(0))=\int_0^{\mathbf{t}}\Big\{\lambda\Big(\upsilon_1\frac{\mathcal{V}\mathcal{T}}{\mathcal{G}^A}+\upsilon_2\mathcal{V}\Big)+\epsilon\frac{\mathcal{G}^L}{\mathcal{G}^A}-\Big(\varrho+\frac{\wp_3}{2}\Big)\Big\}d\mathbf{s}+\wp_3\int_0^{\mathbf{t}}d\mathcal{Q}_3(\mathbf{s})d\mathbf{s}.$$

In view of the strong law of large numbers [52], we have $\lim_{\mathbf{t}\mapsto\infty}\frac{1}{\mathbf{t}}\int_0^{\mathbf{t}}d\mathcal{Q}_3(\mathbf{s})d\mathbf{s}=0,\ (a.s)$.

Taking the superior limit and implementing the stochastic comparison theory yields

$$\begin{aligned}\limsup_{\mathbf{t}\mapsto\infty}\frac{\ln\mathcal{G}^A(\mathbf{t})}{\mathbf{t}}&=\limsup_{\mathbf{t}\mapsto\infty}\frac{1}{\mathbf{t}}\int_0^{\mathbf{t}}\Big\{\lambda\Big(\upsilon_1\frac{\mathcal{V}\mathcal{T}}{\mathcal{G}^A}+\upsilon_2\mathcal{V}\Big)+\epsilon\frac{\mathcal{G}^L}{\mathcal{G}^A}-\Big(\varrho+\frac{\wp_3}{2}\Big)\Big\}d\mathbf{s}-\Big(\varrho+\frac{\wp_3^2}{2}\Big)\\&\leq\frac{\vartheta\lambda\upsilon_2}{\beta}-\Big(\varrho+\frac{\wp_3^2}{2}\Big)\\&\leq\Big(\varrho+\frac{\wp_3^2}{2}\Big)\Big\{\mathbb{R}_0^p-1\Big\}<0\ (a.s).\end{aligned}$$

It follows that $\lim_{\mathbf{t}\mapsto\infty}\mathcal{G}^A(\mathbf{t})=0,\ (a.s)$.

A simple computation reduces (2.12) as

$$\langle\mathcal{V}(\mathbf{t})\rangle=\frac{\vartheta}{\beta}-\frac{1}{\beta}\Big\{\frac{\mathcal{V}(\mathbf{t})-\mathcal{V}(0)}{\mathbf{t}}+\upsilon_1\langle\mathcal{V}(\mathbf{t})\mathcal{T}(\mathbf{t})\rangle+\upsilon_2\langle\mathcal{V}(\mathbf{t})\mathcal{G}^A(\mathbf{t})\rangle+\upsilon_3\langle\mathcal{V}(\mathbf{t})\mathcal{U}^A(\mathbf{t})\rangle-\frac{\wp_1}{\mathbf{t}}\int_0^{\mathbf{t}}\mathcal{V}(s_1)d\mathcal{Q}_1(s_1)\Big\}.$$

Therefore, we have $\lim_{\mathbf{t}\mapsto\infty}\mathcal{V}(\mathbf{t})=\frac{\vartheta}{\beta},\ (a.s)$.

Additionally, we will demonstrate that $\lim_{\mathbf{t}\mapsto\infty}\mathcal{G}^L(\mathbf{t})=0,\ a.s.,\ \lim_{\mathbf{t}\mapsto\infty}\mathcal{U}^L(\mathbf{t})=\frac{\tau}{\vartheta+\lambda_1},\ a.s.,\ \lim_{\mathbf{t}\mapsto\infty}\mathcal{U}^A(\mathbf{t})=0,\ a.s.,\ \lim_{\mathbf{t}\mapsto\infty}\mathcal{T}(\mathbf{t})=0,\ a.s.$, and $\lim_{\mathbf{t}\mapsto\infty}\mathcal{Q}(\mathbf{t})=0,\ a.s.$

This entails that infection extermination is determined by the setting's significance $\mathbb{R}_0^s$, that is, if $\mathbb{R}_0^s<1$. As a result, the infection will eventually become extinct.

2.4. Ergodicity and stationary distribution

Regardless of the dearth of a chronic stable state position in the random system (2.3), we desire to explore the existence of an ESD (stochastic positive equilibrium), which would indicate disease perseverance more thoroughly. First, we offer some of the consequences of Has'minskii's theory. Additional details are accessible at [51].

Consider that there is a homogeneous Markov technique $\tilde{Q}(\mathbf{t})$ in ϑ (the $\mathfrak{d}$-dimensional Euclidean space) that efficiently tackles the stochastic DE described as:

$$d\tilde{Q}(\mathbf{t}) = h_1(\mathbf{y})d\mathbf{t} + \sum_{\iota=1}^{n_1} g_\iota(\tilde{Q})d\mathcal{Q}_\iota(\mathbf{t}). \tag{2.13}$$

The diffusion matrix $A_1(\mathbf{y}) = (a_{\iota\Bbbk}(\mathbf{y}))$ and $a_{\iota\Bbbk}(\mathbf{y}) = \sum_{\omega_1=1}^{n_1} g_{\omega_1}^{(\iota)}(\mathbf{y})g_{\omega_1}^{(\Bbbk)}(\mathbf{y})$.

Lemma 2.2. *([51]) Let us assume a bounded region $\mathcal{U} \subset \Lambda_\mathfrak{d}$ containing a regular boundary Γ such that*
(Z_1) A positive number $\mathbf{Z}$ such that $\sum_{\iota,\Bbbk=1}^{\mathfrak{d}} a_{\iota\Bbbk}(\mathbf{y})\mathbf{t}_\iota\mathbf{t}_\Bbbk \geq \mathbf{Z}|\mathbf{t}|^2,\ \mathbf{y} \in \mathcal{U},\ \mathbf{t} \in \mathbb{R}^\mathfrak{d}$.
(Z_2) $\exists$ a non-negative $\mathbb{C}^2$-mapping $\mathcal{H}$ such that $\mathcal{LH}$ is negative for some $\mathbf{y} \in \Lambda_\mathfrak{d} \setminus \mathcal{U}$ (specifically $\mathcal{LH} \leq -1$, every $\mathbf{y} \in \Lambda_\mathfrak{d} \setminus \mathcal{U}$), then the Markov process $\tilde{Q}(\mathbf{t})$ has only one ESD $\omega_2(.)$, and

$$\mathcal{T}\Big\{\lim_{\mathsf{T}\mapsto\infty}\frac{1}{\mathsf{T}}\int_0^{\mathsf{T}} f_1(\tilde{Q}(\mathbf{t}))d\mathbf{t} = \int_{\varkappa_\mathfrak{d}} f_1(\mathbf{y})\omega_2(d\mathbf{y}) = 1\Big\}, \tag{2.14}$$

holds $\forall\ \mathbf{y} \in \Lambda_\mathfrak{d}$, where $f_1(.)$ is an integrable function with respect to the measure ω_2.

We introduce a threshold

$$\mathbb{R}_0^s = \frac{\upsilon_2\lambda(1-\lambda)}{(\beta+\frac{\wp_1^2}{2})(\epsilon+\xi+\frac{\wp_2^2}{2})(\varrho+\frac{\wp_3^2}{2})(\rho+\frac{\wp_6^2}{2})(\varkappa+\frac{\wp_7^2}{2})}.$$

Furthermore, we will prove prerequisites that ensure the existence of an ESD based on Has'minskii's theorem.

Theorem 2.3. *If $\mathbb{R}_0^s > 1$, then for an ICs $\tilde{\mho}(0) \in \mathbf{R}_+^7$, the system* (2.3) *has only one stationary distribution $\omega_2(.)$ and has the ergodicity.*

Proof. To prove the argument 2.3, straightforwardly examine suppositions (Z_1) and (Z_2) in Lemma 2.2. For this, we construct a suitable Lyapunov mapping F and suppose a closed set $\mathcal{U}_\epsilon \setminus \mathbf{R}_+^7$ such that $\sup_{\tilde{\mho}\in\mathcal{U}_\epsilon\setminus\mathbf{R}_+^7}\mathcal{L}F$ is negative to examine the suitability of (Z_2) in Lemma 2.2.
Next we aim to introduce a non-negative $\mathbb{C}^2$-mapping $\mathcal{H} : \mathbb{R}_+^7 \mapsto \mathbb{R}_+$ as

$$\mathcal{H}_1 = \mathcal{V} + \mathcal{G}^L + \mathcal{G}^A + \mathcal{U}^L + \mathcal{U}^A + \mathcal{T} + \mathcal{Q} - \chi_1\ln\mathcal{V} - \chi_2\ln\mathcal{G}^L - \chi_3\ln\mathcal{G}^A - \chi_4\ln\mathcal{T} - \chi_5\ln\mathcal{Q}, \tag{2.15}$$

here the positive constants $\chi_1, \chi_2, \chi_3, \chi_4$ and χ_5 can be evaluated later. By applying Itô's approach and the suggested framework, we accomplish the following results (2.3) as

$$\mathcal{L}(\mathcal{V} + \mathcal{G}^L + \mathcal{G}^A + \mathcal{U}^L + \mathcal{U}^A + \mathcal{T} + \mathcal{Q}) = \vartheta - \beta(\mathcal{V} + \mathcal{G}^L + \mathcal{G}^A + \mathcal{U}^L + \mathcal{U}^A + \mathcal{T} + \mathcal{Q}),$$

$$\ln(-\mathcal{V}) = -\frac{\vartheta}{\mathcal{V}} + \beta - \upsilon_1\mathcal{T} - \upsilon_2\mathcal{G}^A - \upsilon_3\mathcal{U}^A + \frac{\wp_1^2}{2},$$
$$\ln(-\mathcal{G}^L) = -(1-\lambda)\Big(\upsilon_1\frac{\mathcal{V}\mathcal{T}}{\mathcal{G}^L} + \upsilon_2\frac{\mathcal{V}\mathcal{G}^A}{\mathcal{G}^L}\Big) + (\epsilon + \xi) + \frac{\wp_2^2}{2},$$
$$\ln(-\mathcal{G}^A) = -\lambda\Big(\upsilon_1\frac{\mathcal{V}\mathcal{T}}{\mathcal{G}^A} + \upsilon_2\mathcal{V}\Big) - \epsilon\frac{\mathcal{G}^L}{\mathcal{G}^A} + \varrho + \frac{\wp_3^2}{2},$$
$$\ln(-\mathcal{U}^L) = -\tau\upsilon_3\frac{\mathcal{V}\mathcal{U}^A}{\mathcal{U}^L} + (\sigma + \varsigma) + \frac{\wp_4^2}{2},$$
$$\ln(-\mathcal{U}^A) = -\sigma\frac{\mathcal{U}^L}{\mathcal{U}^A} + \phi + \frac{\wp_5^2}{2},$$
$$\ln(-\mathcal{T}) = -\omega_1\frac{\mathcal{G}^A}{\mathcal{T}} + \rho + \omega_2\mathcal{Q} + \frac{\wp_6^2}{2},$$
$$\ln(-\mathcal{Q}) = -\delta\mathcal{T} + \varkappa + \frac{\wp_7^2}{2}. \tag{2.16}$$

Therefore, we have

$$\begin{aligned}\mathcal{L}\mathcal{H}_1(\tilde{\mho}(\mathbf{t})) \quad &= -\beta(\mathcal{V} + \mathcal{G}^L + \mathcal{G}^A + \mathcal{U}^L + \mathcal{U}^A + \mathcal{T} + \mathcal{Q}) - \frac{\chi_1\vartheta}{\mathcal{V}} - \chi_1\upsilon_1\mathcal{T} - \chi_1\upsilon_2\mathcal{G}^A - \chi_1\upsilon_3\mathcal{U}^A \\ &\quad + \chi_1\Big(\beta + \frac{\wp_1^2}{2}\Big) + \chi_2\Big(\epsilon + \xi + \frac{\wp_2^2}{2}\Big) + \chi_3\Big(\varrho + \frac{\wp_3^2}{2}\Big) + \chi_4\Big(\rho + \frac{\wp_6^2}{2}\Big) + \chi_5\Big(\varkappa + \frac{\wp_7^2}{2}\Big) + \\ &\quad + \lambda\upsilon_2\mathcal{V} + (1-\lambda)\upsilon_1\mathcal{V}, \end{aligned} \tag{2.17}$$

which gives

$$\begin{aligned}\mathcal{L}\mathcal{H}_1(\tilde{\mho}(\mathbf{t})) \quad &\leq -7\Big\{\beta(\mathcal{V} + \mathcal{G}^L + \mathcal{G}^A + \mathcal{U}^L + \mathcal{U}^A + \mathcal{T} + \mathcal{Q}) - \frac{\chi_1\vartheta}{\mathcal{V}} - \chi_1\upsilon_1\mathcal{T} - \chi_1\upsilon_2\mathcal{G}^A - \chi_1\upsilon_3\mathcal{U}^A + \\ &\quad + \lambda\upsilon_2\mathcal{V} + (1-\lambda)\upsilon_1\frac{\mathcal{V}}{\beta(\mathcal{V} + \mathcal{G}^L + \mathcal{G}^A + \mathcal{U}^L + \mathcal{U}^A + \mathcal{T} + \mathcal{Q})}\Big\}^{1/7} \\ &\quad + \chi_1\Big(\beta + \frac{\wp_1^2}{2}\Big) + \chi_2\Big(\epsilon + \xi + \frac{\wp_2^2}{2}\Big) + \chi_3\Big(\varrho + \frac{\wp_3^2}{2}\Big) + \chi_4\Big(\rho + \frac{\wp_6^2}{2}\Big) + \chi_5\Big(\varkappa + \frac{\wp_7^2}{2}\Big) + \vartheta. \end{aligned} \tag{2.18}$$

Choosing

$$\chi_1\Big(\beta + \frac{\wp_1^2}{2}\Big) = \chi_2\Big(\epsilon + \xi + \frac{\wp_2^2}{2}\Big) = \chi_3\Big(\varrho + \frac{\wp_3^2}{2}\Big) = \chi_4\Big(\rho + \frac{\wp_6^2}{2}\Big) = \chi_5\Big(\varkappa + \frac{\wp_7^2}{2}\Big) = \vartheta. \tag{2.19}$$

Indicating

$$\chi_1 = \frac{\vartheta}{\beta + \frac{\wp_1^2}{2}},\ \chi_2 = \frac{\vartheta}{\epsilon + \xi + \frac{\wp_2^2}{2}},\ \chi_3 = \frac{\vartheta}{\varrho + \frac{\wp_3^2}{2}},\ \chi_4 = \frac{\vartheta}{\rho + \frac{\wp_6^2}{2}},\ \chi_5 = \frac{\vartheta}{\varkappa + \frac{\wp_7^2}{2}}. \tag{2.20}$$

Therefore, we get

$$\mathcal{L}\mathcal{H}_1(\tilde{\mho}(\mathbf{t})) \quad \leq -7\Big[\Big(\frac{\vartheta^7\upsilon_2\lambda(1-\lambda)}{(\beta + \frac{\wp_1^2}{2})(\epsilon + \xi + \frac{\wp_2^2}{2})(\varrho + \frac{\wp_3^2}{2})(\rho + \frac{\wp_6^2}{2})(\varkappa + \frac{\wp_7^2}{2})}\Big)^{1/7} - \vartheta\Big] + \chi_1\frac{\vartheta}{\mathcal{V}}$$

$$\leq -4\vartheta[(\mathbb{R}_0^s)^{1/4} - 1] + \chi_1 \frac{\chi}{\mathcal{V}}. \tag{2.21}$$

Additionally, we express

$$\begin{aligned}\mathcal{H}_2(\tilde{\mho}(\mathbf{t})) &= \chi_6(\mathcal{V} + \mathcal{G}^L + \mathcal{G}^A + \mathcal{U}^L + \mathcal{U}^A + \mathcal{T} + \mathcal{Q} - \chi_1 \ln \mathcal{V} - \chi_2 \ln \mathcal{G}^L - \chi_3 \ln \mathcal{G}^A - \chi_4 \ln \mathcal{T} - \chi_5 \ln \mathcal{Q}) \\ &\quad - \ln \mathcal{V} - \ln \mathcal{U}^L - \ln \mathcal{U}^A + \mathcal{V} + \mathcal{G}^L + \mathcal{G}^A + \mathcal{U}^L + \mathcal{U}^A + \mathcal{T} + \mathcal{Q} \\ &= (\chi_6 + 1)(\mathcal{V} + \mathcal{G}^L + \mathcal{G}^A + \mathcal{U}^L + \mathcal{U}^A) - (\chi_6\chi_1 + 1) \ln \mathcal{V} - \chi_6\chi_2 \ln \mathcal{G}^L - \chi_6\chi_3 \ln \mathcal{G}^A \\ &\quad -\chi_6\chi_4 \ln \mathcal{T} - \chi_6\chi_5 \ln \mathcal{Q} - \ln \mathcal{U}^L - \ln \mathcal{U}^A.\end{aligned} \tag{2.22}$$

In this case, $\chi_4 > 0$ is a constant that will be identified later on. As a result, it is critical for displaying

$$\lim \inf_{(\tilde{\mho}(\mathbf{t}))\in\mathbb{R}_+^7\setminus\mathcal{U}_{\omega_1}} \mathcal{H}_2(\tilde{\mho}(\mathbf{t})) = +\infty, \ \ as\ \omega_1 \mapsto \infty, \tag{2.23}$$

thus, $\mathcal{U}_{\omega_1} = (\frac{1}{\omega_1}, \omega_1) \times (\frac{1}{\omega_1}, \omega_1) \times (\frac{1}{\omega_1}, \omega_1) \times (\frac{1}{\omega_1}, \omega_1) \times (\frac{1}{\omega_1}, \omega_1) \times (\frac{1}{\omega_1}, \omega_1) \times (\frac{1}{\omega_1}, \omega_1)$. Moreover, we exhibit that $\mathcal{H}_2(\tilde{\mho}(\mathbf{t}))$ has unique minimum value $\mathcal{H}_2(\tilde{\mho}(0))$.
The partial derivative of $\mathcal{H}_2(\tilde{\mho}(\mathbf{t}))$ in respect to $\mathcal{V}$, $\mathcal{G}^L$, $\mathcal{G}^A$, $\mathcal{U}^L$, $\mathcal{U}^A$, $\mathcal{T}$, $\mathcal{Q}$, is as follows:

$$\begin{aligned}&\frac{\partial \mathcal{H}_2(\tilde{\mho}(\mathbf{t}))}{\partial \mathcal{V}} = 1 + \chi_6 - \frac{\chi_1\chi_6 + 1}{\mathcal{V}}, \quad \frac{\partial \mathcal{H}_2(\tilde{\mho}(\mathbf{t}))}{\partial \mathcal{G}^L} = 1 + \chi_6 - \frac{\chi_6\chi_2}{\mathcal{G}^L} \\ &\frac{\partial \mathcal{H}_2(\tilde{\mho}(\mathbf{t}))}{\partial \mathcal{G}^A} = 1 + \chi_6 - \frac{\chi_6\chi_3}{\mathcal{G}^A}, \quad \frac{\partial \mathcal{H}_2(\tilde{\mho}(\mathbf{t}))}{\partial \mathcal{U}^L} = 1 + \chi_6 - \frac{1}{\mathcal{U}^L}, \\ &\frac{\partial \mathcal{H}_2(\tilde{\mho}(\mathbf{t}))}{\partial \mathcal{U}^A} = 1 + \chi_4 - \frac{1}{\mathcal{U}^A}, \quad \frac{\partial \mathcal{H}_2(\tilde{\mho}(\mathbf{t}))}{\partial \mathcal{T}} = 1 + \chi_6 - \frac{\chi_6\chi_4}{\mathcal{T}}, \\ &\frac{\partial \mathcal{H}_2(\tilde{\mho}(\mathbf{t}))}{\partial \mathcal{Q}} = 1 + \chi_6 - \frac{\chi_5\chi_6}{\mathcal{Q}}.\end{aligned} \tag{2.24}$$

Clearly, it can be revealed that $\mathcal{H}_2$ has a different stagnation point, identified by the subsequent formula:

$$\tilde{\mho}(0) = \Big(\frac{\chi_1\chi_6 + 1}{1 + \chi_6}, \frac{\chi_2\chi_6}{1 + \chi_6}, \frac{\chi_3\chi_6}{1 + \chi_6}, \frac{1}{1 + \chi_6}, \frac{1}{1 + \chi_6}, \frac{\chi_4\chi_6}{1 + \chi_6}, \frac{\chi_5\chi_6}{1 + \chi_6}\Big). \tag{2.25}$$

Also, the Hessian matrix of $\mathcal{H}_2(\tilde{\mho}(\mathbf{t}))$ at $\tilde{\mho}(0)$ is

$$\mathcal{P} = \begin{bmatrix} \frac{1+\chi_1\chi_6}{\mathcal{V}^2(0)} & 0 & 0 & 0 & 0 & 0 & 0 \\ 0 & \frac{\chi_2\chi_6}{\mathcal{G}^{2L}(0)} & 0 & 0 & 0 & 0 & 0 \\ 0 & 0 & \frac{\chi_3\chi_6}{\mathcal{G}^{2A}(0)} & 0 & 0 & 0 & 0 \\ 0 & 0 & 0 & \frac{1}{\mathcal{U}^{2L}(0)} & 0 & 0 & 0 \\ 0 & 0 & 0 & 0 & \frac{1}{\mathcal{U}^{2A}(0)} & 0 & 0 \\ 0 & 0 & 0 & 0 & 0 & \frac{\chi_4\chi_6}{\mathcal{T}(0)} & 0 \\ 0 & 0 & 0 & 0 & 0 & 0 & \frac{\chi_5\chi_6}{\mathcal{Q}(0)} \end{bmatrix}. \tag{2.26}$$

It is obvious that the aforementioned matrix is positive definite. As a result, $\mathcal{H}_2(\tilde{\mho}(\mathbf{t}))$ has a minimum of $\mathcal{H}_2(\tilde{\mho}(0))$.

Considering (2.23) and by the continuity of $\mathcal{H}_2(\tilde{\mathfrak{O}}(\mathbf{t}))$, we can determine from this $\mathcal{H}_2(\tilde{\mathfrak{O}}(\mathbf{t}))$ has at least one value $\mathcal{H}_2(\tilde{\mathfrak{O}}(0))$ stayed in $\mathbb{R}^7_+$.
Analogously, we introduce a non-negative $\mathbb{C}^2$-mapping $\mathcal{H}_3 : \mathbb{R}^7_+ \mapsto \mathbb{R}_+$ as follows:

$$\mathcal{H}_3(\tilde{\mathfrak{O}}(\mathbf{t})) = \mathcal{H}_2(\tilde{\mathfrak{O}}(\mathbf{t})) - \mathcal{H}_2(\tilde{\mathfrak{O}}(0)). \tag{2.27}$$

Utilizing Itô's technique and proposed model (2.3) yields

$$\begin{aligned}\mathcal{L}\mathcal{H}_3(\tilde{\mathfrak{O}}(\mathbf{t})) \quad &\leq \chi_6\Big\{-7\vartheta[(\mathbb{R}_0^s)^{1/7}-1]+\chi_1\frac{\vartheta}{\mathcal{V}}\Big\}-\frac{\vartheta}{\mathcal{V}}+\beta-\upsilon_1\mathcal{T}-\upsilon_2\mathcal{G}^A-\upsilon_3\mathcal{U}^A+\frac{\wp_1^2}{2}\\ &-(1-\lambda)\Big(\upsilon_1\frac{\mathcal{V}\mathcal{T}}{\mathcal{G}^L}+\upsilon_2\frac{\mathcal{V}\mathcal{G}^A}{\mathcal{G}^L}\Big)+(\epsilon+\xi)+\frac{\wp_2^2}{2}-\lambda\Big(\upsilon_1\frac{\mathcal{V}\mathcal{T}}{\mathcal{G}^A}+\upsilon_2\mathcal{V}\Big)-\epsilon\frac{\mathcal{G}^L}{\mathcal{G}^A}\\ &+\varrho+\frac{\wp_3^2}{2}-\omega_1\frac{\mathcal{G}^A}{\mathcal{T}}+\rho+\omega_2\mathcal{Q}+\frac{\wp_6^2}{2}-\delta\mathcal{T}+\varkappa+\frac{\wp_7^2}{2}+\vartheta-\beta(\mathcal{V}+\mathcal{G}^L+\mathcal{G}^A+\mathcal{U}^L+\mathcal{U}^A),\end{aligned} \tag{2.28}$$

As an outcome, the preceding idea can be expressed as

$$\begin{aligned}\mathcal{L}\mathcal{H}_3(\tilde{\mathfrak{O}}(\mathbf{t})) \quad &\leq \chi_6\delta_7+(\chi_1\chi_6-1)\frac{\vartheta}{\mathcal{V}}+\beta-\upsilon_1\mathcal{T}-\upsilon_2\mathcal{G}^A-\upsilon_3\mathcal{U}^A+\frac{\wp_1^2}{2}\\ &-(1-\lambda)\Big(\upsilon_1\frac{\mathcal{V}\mathcal{T}}{\mathcal{G}^L}+\upsilon_2\frac{\mathcal{V}\mathcal{G}^A}{\mathcal{G}^L}\Big)+(\epsilon+\xi)+\frac{\wp_2^2}{2}-\lambda\Big(\upsilon_1\frac{\mathcal{V}\mathcal{T}}{\mathcal{G}^A}+\upsilon_2\mathcal{V}\Big)-\epsilon\frac{\mathcal{G}^L}{\mathcal{G}^A}\\ &+\varrho+\frac{\wp_3^2}{2}-\omega_1\frac{\mathcal{G}^A}{\mathcal{T}}+\rho+\omega_2\mathcal{Q}+\frac{\wp_6^2}{2}-\delta\mathcal{T}+\varkappa+\frac{\wp_7^2}{2}+\vartheta-\beta(\mathcal{V}+\mathcal{G}^L+\mathcal{G}^A+\mathcal{U}^L+\mathcal{U}^A),\end{aligned} \tag{2.29}$$

where $\delta_7 = 7\vartheta[(\mathbb{R}_0^s)^{1/7}-1] > 0$. A group's description is supplied by

$$\mathcal{W}^\diamond = \Big\{\mathcal{V}\in(\epsilon_1,1/\epsilon_2),\mathcal{G}^L\in(\epsilon_1,1/\epsilon_2),\mathcal{G}^A\in(\epsilon_1,1/\epsilon_2),\mathcal{U}^L\in(\epsilon_1,1/\epsilon_2),\mathcal{U}^A\in(\epsilon_1,1/\epsilon_2),\mathcal{T}\in(\epsilon_1,1/\epsilon_2),\mathcal{Q}\in(\epsilon_1,1/\epsilon_2)\Big\} \tag{2.30}$$

where ϵ_ι, $\iota = 1, 2$ are constants, which are very small and are likely to be noticed afterward. We will break up the entire $\mathbb{R}^7_+ \setminus \mathcal{W}^\diamond$ into ten regions:

$$\begin{aligned}&\mathcal{W}_1^\diamond = \{(\tilde{\mathfrak{O}}(\mathbf{t}))\in\mathbb{R}^7_+, 0<\mathcal{V}\leq\epsilon_1\},\quad \mathcal{W}_2^\diamond = \{(\tilde{\mathfrak{O}}(\mathbf{t}))\in\mathbb{R}^7_+, 0<\mathcal{G}^L\leq\epsilon_2, \mathcal{V}>\epsilon_2\},\\ &\mathcal{W}_3^\diamond = \{(\tilde{\mathfrak{O}}(\mathbf{t}))\in\mathbb{R}^7_+, 0<\mathcal{G}^A\leq\epsilon_1, \mathcal{G}^L>\epsilon_2\},\quad \mathcal{W}_4^\diamond = \{(\tilde{\mathfrak{O}}(\mathbf{t}))\in\mathbb{R}^7_+, 0<\mathcal{U}^L\leq\epsilon_1, \mathcal{G}^A>\epsilon_2\},\\ &\mathcal{W}_5^\diamond = \{(\tilde{\mathfrak{O}}(\mathbf{t}))\in\mathbb{R}^7_+, 0<\mathcal{U}^A\leq\epsilon_1, \mathcal{U}^L>\epsilon_2\},\quad \mathcal{W}_6^\diamond = \{(\tilde{\mathfrak{O}}(\mathbf{t}))\in\mathbb{R}^7_+, 0<\mathcal{T}\leq\epsilon_1, \mathcal{U}^A>\epsilon_2\},\\ &\mathcal{W}_7^\diamond = \{(\tilde{\mathfrak{O}}(\mathbf{t}))\in\mathbb{R}^7_+, 0<\mathcal{Q}\leq\epsilon_1, \mathcal{T}>\epsilon_2\},\quad \mathcal{W}_8^\diamond = \{(\tilde{\mathfrak{O}}(\mathbf{t}))\in\mathbb{R}^7_+, \mathcal{V}\geq\frac{1}{\epsilon_2}\},\\ &\mathcal{W}_9^\diamond = \{(\tilde{\mathfrak{O}}(\mathbf{t}))\in\mathbb{R}^7_+, \mathcal{G}^L\geq\frac{1}{\epsilon_2}\},\quad \mathcal{W}_{10}^\diamond = \{(\tilde{\mathfrak{O}}(\mathbf{t}))\in\mathbb{R}^7_+, \mathcal{G}^L\geq\frac{1}{\epsilon_2}\},\\ &\mathcal{W}_{11}^\diamond = \{(\tilde{\mathfrak{O}}(\mathbf{t}))\in\mathbb{R}^7_+, \mathcal{U}^L\geq\frac{1}{\epsilon_2}\},\quad \mathcal{W}_{12}^\diamond = \{(\tilde{\mathfrak{O}}(\mathbf{t}))\in\mathbb{R}^7_+, \mathcal{U}^A\geq\frac{1}{\epsilon_2}\},\\ &\mathcal{W}_{13}^\diamond = \{(\tilde{\mathfrak{O}}(\mathbf{t}))\in\mathbb{R}^7_+, \mathcal{T}\geq\frac{1}{\epsilon_2}\},\quad \mathcal{W}_{14}^\diamond = \{(\tilde{\mathfrak{O}}(\mathbf{t}))\in\mathbb{R}^7_+, \mathcal{Q}\geq\frac{1}{\epsilon_2}\}.\end{aligned} \tag{2.31}$$

Likewise, we will demonstrate that $\mathcal{L}\mathcal{H}_3((\tilde{\mathfrak{O}}(\mathbf{t})) < 0$, which is similar to displaying it within the earlier specified fourteen categories.

Case I. If $\tilde{\mho}(\mathbf{t}) \in \mathcal{W}_1^{\diamond}$, in view of (2.29), it gives

$$\begin{aligned}
\mathcal{L}\mathcal{H}_3(\tilde{\mho}(\mathbf{t})) \quad &\leq -\chi_6\delta_7 + (\chi_1\chi_6 - 1)\frac{\vartheta}{\mathcal{V}} + \beta - \upsilon_1\mathcal{T} - \upsilon_2\mathcal{G}^A - \upsilon_3\mathcal{U}^A + \frac{\wp_1^2}{2} \\
&\quad -(1-\lambda)\Big(\upsilon_1\frac{\mathcal{V}\mathcal{T}}{\mathcal{G}^L} + \upsilon_2\frac{\mathcal{V}\mathcal{G}^A}{\mathcal{G}^L}\Big) + (\epsilon + \xi) + \frac{\wp_2^2}{2} - \lambda\Big(\upsilon_1\frac{\mathcal{V}\mathcal{T}}{\mathcal{G}^A} + \upsilon_2\mathcal{V}\Big) - \epsilon\frac{\mathcal{G}^L}{\mathcal{G}^A} \\
&\quad +\varrho + \frac{\wp_3^2}{2} - \omega_1\frac{\mathcal{G}^A}{\mathcal{T}} + \rho + \omega_2\mathcal{Q} + \frac{\wp_6^2}{2} - \delta\mathcal{T} + \varkappa + \frac{\wp_7^2}{2} + \vartheta - \beta(\mathcal{V} + \mathcal{G}^L + \mathcal{G}^A + \mathcal{U}^L + \mathcal{U}^A) \\
&\leq (\chi_1\chi_6 - 1)\frac{\vartheta}{\epsilon_1} + \beta - \upsilon_1\mathcal{T} - \upsilon_2\mathcal{G}^A - \upsilon_3\mathcal{U}^A + \frac{\wp_1^2}{2} \\
&\quad -(1-\lambda)\Big(\upsilon_1\frac{\mathcal{V}\mathcal{T}}{\mathcal{G}^L} + \upsilon_2\frac{\mathcal{V}\mathcal{G}^A}{\mathcal{G}^L}\Big) + (\epsilon + \xi) + \frac{\wp_2^2}{2} - \lambda\Big(\upsilon_1\frac{\mathcal{V}\mathcal{T}}{\mathcal{G}^A} + \upsilon_2\mathcal{V}\Big) - \epsilon\frac{\mathcal{G}^L}{\mathcal{G}^A} \\
&\quad +\varrho + \frac{\wp_3^2}{2} - \omega_1\frac{\mathcal{G}^A}{\mathcal{T}} + \rho + \omega_2\mathcal{Q} + \frac{\wp_6^2}{2} - \delta\mathcal{T} + \varkappa + \frac{\wp_7^2}{2} + \vartheta.
\end{aligned}$$

Selecting $\epsilon_1 > 0$, produces $\mathcal{L}\mathcal{H}_3(\tilde{\mho}(\mathbf{t})) < 0$ each $\tilde{\mho}(\mathbf{t}) \in \mathcal{W}_1^{\diamond}$. Repeating the same procedure, we can get the other cases immediately.

As a consequence, we demonstrate that an integer $\mathcal{P} > 0$ ensures

$$\mathcal{L}\mathcal{H}_3(\tilde{\mho}(\mathbf{t})) < -\mathcal{P} < 0 \;\; \forall \tilde{\mho}(\mathbf{t}) \in \mathbb{R}_+^7 \setminus \mathcal{W}^{\diamond}.$$

Therefore, we have

$$\begin{aligned}
d\mathcal{H}_3(\tilde{\mho}(\mathbf{t})) \quad &< -\mathcal{P}d\mathbf{t} + [(\chi_6 + 1)\mathcal{V} - (1 + \chi_1\chi_6)\wp_1]d\mathcal{Q}_1(\mathbf{t}) + [(\chi_6 + 1)\mathcal{G}^L - \chi_2\chi_6\wp_2]d\mathcal{Q}_2(\mathbf{t}) \\
&\quad +[(\chi_6 + 1)\mathcal{G}^A - \chi_3\chi_6\wp_3]d\mathcal{Q}_3(\mathbf{t}) + [(\chi_6 + 1)\mathcal{Y}^L - \wp_4]d\mathcal{Q}_4(\mathbf{t}) + [(\chi_6 + 1)\mathcal{U}^A - \wp_5]d\mathcal{Q}_5(\mathbf{t}) \\
&\quad +[(\chi_6 + 1)\mathcal{T} - \chi_4\chi_6\wp_6]d\mathcal{Q}_6(\mathbf{t}) + [(\chi_6 + 1)\mathcal{Q} - \chi_6\chi_5\wp_6]d\mathcal{Q}_7(\mathbf{t}). \qquad (2.32)
\end{aligned}$$

Consider that $((\tilde{\mho}(\mathbf{t}))(0)) = (\mathbf{w}_1, \mathbf{w}_2, \mathbf{w}_3, \mathbf{w}_4, \mathbf{w}_5, \mathbf{w}_6, \mathbf{w}_7) = \mathbf{w} \in \mathbb{R}_+^7 \setminus \mathcal{W}^{\diamond}$ and $\xi^{\mathbf{w}}$ is the duration wherein a sequence of events starting at $\mathbf{w}$ results in the subsequent set $\mathcal{W}^{\diamond}$

$$\xi_n = \inf\{\mathbf{t} : |\mho(\mathbf{t})| = \mathfrak{n}\} \;\; and \;\; \xi^{(n)}(\mathbf{t}) = \min\{\xi^{\mathbf{w}}, \mathbf{t}, \xi_{\mathfrak{n}}\}.$$

The consequence that follows can be produced by integrating both sides of the inequality (2.32) from 0 to $\xi^{(n)}(\mathbf{t})$), applying expectation with the use of Dynkin's computation, we have:

$$\begin{aligned}
&\mathbf{E}\mathcal{H}_3(\mathcal{V}(\xi^{(n)}(\mathbf{t})), \mathcal{G}^L(\xi^{(n)}(\mathbf{t})), \mathcal{G}^A(\xi^{(n)}(\mathbf{t})), \mathcal{U}^L(\xi^{(n)}(\mathbf{t})), \mathcal{U}^A(\xi^{(n)}(\mathbf{t}), \mathcal{T}(\xi^{(n)}(\mathbf{t}), \mathcal{Q}(\xi^{(n)}(\mathbf{t})) - \mathcal{H}_3(\mathbf{w})) \\
&= \mathbf{E}\int_0^{\xi^{(n)}(\mathbf{t})} \mathcal{L}\mathcal{H}_3(\mathcal{V}(\mathbf{w}), \mathcal{G}^L(\mathbf{w}), \mathcal{G}^A(\mathbf{w}), \mathcal{U}^L(\mathbf{w}), \mathcal{U}^A(\mathbf{w}), \mathcal{T}(\mathbf{w}), \mathcal{Q}(\mathbf{w}))d\mathbf{w} \\
&\leq \mathbf{E}\int_0^{\xi^{(n)}(\mathbf{t})} -\mathcal{P}d\mathbf{w} = -\mathcal{P}\mathbf{E}\xi^{(n)}(\mathbf{t}).
\end{aligned}$$

$\mathcal{H}_3(\mathbf{w})$ is a non-negative number, hence

$$\mathbf{E}\xi^{(n)}(\mathbf{t}) \leq \frac{\mathcal{H}_3(\mathbf{w})}{\mathcal{P}}.$$

Thus, we deduce $\mathcal{T}\{\xi_\epsilon = \infty\}$, the desired result of Theorem 2.3.

Conversely, the scheme established in (2.3) can be considered regular. For this, considering $\mathbf{t} \mapsto \infty$ and $n \mapsto \infty$, we will get $\xi^{(n)}(\mathbf{t}) \mapsto \xi^{\mathbf{w}}$ $(a.s)$.

Thus, employing Fatou's lemma, we attain

$$\mathbf{E}\xi^{(n)}(\mathbf{t}) \leq \frac{\mathcal{H}_3(\mathbf{w})}{\mathcal{P}} < \infty.$$

Clearly, $\sup_{\mathbf{w}\in C} \mathbf{E}\xi^{\mathbf{w}} < \infty$. Here, $C \in \mathbb{R}_+^7$ is a compact subset. It confirms the hypothesis (Z_2) of Lemma 2.1.

Also, the model's (2.3) diffusion matrix is

$$\mathcal{P} = \begin{bmatrix} \wp_1^2\mathcal{V}^2 & 0 & 0 & 0 & 0 & 0 & 0 \\ 0 & \wp_2^2\mathcal{G}^{2L} & 0 & 0 & 0 & 0 & 0 \\ 0 & 0 & \wp_3^2\mathcal{G}^{2A} & 0 & 0 & 0 & 0 \\ 0 & 0 & 0 & \wp_4^2\mathcal{U}^{2L} & 0 & 0 & 0 \\ 0 & 0 & 0 & 0 & \wp_5^2\mathcal{U}^{2A} & 0 & 0 \\ 0 & 0 & 0 & 0 & 0 & \wp_6^2\mathcal{T} & 0 \\ 0 & 0 & 0 & 0 & 0 & 0 & \wp_7^2\mathcal{Q} \end{bmatrix}.$$

Selecting $\mathcal{M} = \min_{(\tilde{\mho}(\mathbf{t}))\in\bar{\mathcal{W}}^\diamond\in\mathbb{R}_+^7} \{\wp_1^2\mathcal{V}^2, \wp_2^2\mathcal{G}^{2L}, \wp_3^2\mathcal{G}^{2A}, \wp_4^2\mathcal{U}^{2L}, \wp_5^2\mathcal{U}^{2A}, \wp_6^2\mathcal{T}, \wp_7^2\mathcal{Q}\}$, we find

$$\begin{aligned} \sum_{\iota,J=1}^{5} a_{\iota J}(\tilde{\mho}(\mathbf{t}))_{r_\iota r_J} &= \wp_1^2\mathcal{V}^2r_1^2 + \wp_2^2\mathcal{G}^{2L}r_2^2 + \wp_3^2\mathcal{G}^{2A}r_3^2 + \wp_4^2\mathcal{U}^{2L}r_4^2 + \wp_5^2\mathcal{U}^{2A}r_5^2 + \wp_6^2\mathcal{T}r_6^2 + \wp_7^2\mathcal{Q}r_7^2 \\ &\geq \mathcal{M}|r|^2 \quad \forall(\tilde{\mho}(\mathbf{t})) \in \bar{\mathcal{W}}^\diamond, \end{aligned}$$

where $r = (r_1, r_2, r_3, r_4, r_5, r_6, r_7) \in \mathbb{R}_+^7$. This implies that the notion (Z_1) of Lemma 2.1 is also accurate. In accordance to the initial review, Lemma 2.1 indicates that the system (2.3) has a unique ESD.

3. Numerical estimates of HIV-1/HTLV-I system with piecewise derivative

This part consists of the numerical schemes of crossover effects when the differentiation formulations are in integer-order and there are fraction differential formulations via local and non-local memory. The order of the fractional operators lies between 0 and 1.

3.1. Proposed model via power-law kernel

Here, we want to explore the codynamics of the HIV-1/HTLV-I models (2.1) and (2.3) that include responses of immunity and cellular outbreak, including integer-order, power-law and culminating in random procedures. If T is identified as the last phase of dissemination, then the conceptual structure will be constructed in the initial stage employing the integer-order derivative form, followed by the index-law kernel in the next phase, culminating in the random setting in the following steps. Following

that, a numerical convention that clarifies this occurrence is offered as:

$$\begin{cases} \frac{d\mathcal{V}}{d\mathbf{t}} = \vartheta - \beta\mathcal{V} - \upsilon_1\mathcal{V}\mathcal{T} - \upsilon_2\mathcal{V}\mathcal{G}^A - \upsilon_3\mathcal{V}\mathcal{U}^A, \\ \frac{d\mathcal{G}^L}{d\mathbf{t}} = (1-\lambda)(\upsilon_1\mathcal{V}\mathcal{T} + \upsilon_2\mathcal{V}\mathcal{G}^A) - (\epsilon+\xi)\mathcal{G}^L, \\ \frac{d\mathcal{G}^L}{d\mathbf{t}} = \lambda(\upsilon_1\mathcal{V}\mathcal{T} + \upsilon_2\mathcal{V}\mathcal{G}^A) + \epsilon\mathcal{G}^L - \varrho\mathcal{G}^A, \\ \frac{d\mathcal{U}^L}{d\mathbf{t}} = \tau\upsilon_3\mathcal{V}\mathcal{U}^A - (\sigma+\varsigma)\mathcal{U}^L, \ if\ 0 \le \mathbf{t} \le \mathsf{T}_1, \\ \frac{d\mathcal{U}^A}{d\mathbf{t}} = \sigma\mathcal{U}^L - \phi\mathcal{U}^A, \\ \frac{d\mathcal{T}}{d\mathbf{t}} = \omega_1\mathcal{G}^A - \rho\mathcal{T} - \omega_2\mathcal{Q}\mathcal{T}, \\ \frac{dQ}{d\mathbf{t}} = \delta\mathcal{Q}\mathcal{T} - \varkappa\mathcal{Q}. \end{cases} \tag{3.1}$$

$$\begin{cases} {}_0^c\mathbf{D}_{\mathbf{t}}^{\eta}\mathcal{V} = \vartheta - \beta\mathcal{V} - \upsilon_1\mathcal{V}\mathcal{T} - \upsilon_2\mathcal{V}\mathcal{G}^A - \upsilon_3\mathcal{V}\mathcal{U}^A, \\ {}_0^c\mathbf{D}_{\mathbf{t}}^{\eta}\mathcal{G}^L = (1-\lambda)(\upsilon_1\mathcal{V}\mathcal{T} + \upsilon_2\mathcal{V}\mathcal{G}^A) - (\epsilon+\xi)\mathcal{G}^L, \\ {}_0^c\mathbf{D}_{\mathbf{t}}^{\eta}\mathcal{G}^L = \lambda(\upsilon_1\mathcal{V}\mathcal{T} + \upsilon_2\mathcal{V}\mathcal{G}^A) + \epsilon\mathcal{G}^L - \varrho\mathcal{G}^A, \\ {}_0^c\mathbf{D}_{\mathbf{t}}^{\eta}\mathcal{U}^L = \tau\upsilon_3\mathcal{V}\mathcal{U}^A - (\sigma+\varsigma)\mathcal{U}^L, \ if\ \mathsf{T}_1 \le \mathbf{t} \le \mathsf{T}_2, \\ {}_0^c\mathbf{D}_{\mathbf{t}}^{\eta}\mathcal{U}^A = \sigma\mathcal{U}^L - \phi\mathcal{U}^A, \\ {}_0^c\mathbf{D}_{\mathbf{t}}^{\eta}\mathcal{T} = \omega_1\mathcal{G}^A - \rho\mathcal{T} - \omega_2\mathcal{Q}\mathcal{T}, \\ {}_0^c\mathbf{D}_{\mathbf{t}}^{\eta}\mathcal{Q} = \delta\mathcal{Q}\mathcal{T} - \varkappa\mathcal{Q}. \end{cases} \tag{3.2}$$

$$\begin{cases} d\mathcal{V} = [\vartheta - \beta\mathcal{V} - \upsilon_1\mathcal{V}\mathcal{T} - \upsilon_2\mathcal{V}\mathcal{G}^A - \upsilon_3\mathcal{V}\mathcal{U}^A]d\mathbf{t} + \wp_1\mathcal{V}d\mathcal{Q}_1(\mathbf{t}), \\ d\mathcal{G}^L = [(1-\lambda)(\upsilon_1\mathcal{V}\mathcal{T} + \upsilon_2\mathcal{V}\mathcal{G}^A) - (\epsilon+\xi)\mathcal{G}^L]d\mathbf{t} + \wp_2\mathcal{G}^L d\mathcal{Q}_2(\mathbf{t}), \\ d\mathcal{G}^A = [\lambda(\upsilon_1\mathcal{V}\mathcal{T} + \upsilon_2\mathcal{V}\mathcal{G}^A) + \epsilon\mathcal{G}^L - \varrho\mathcal{G}^A]d\mathbf{t} + \wp_3\mathcal{G}^A d\mathcal{Q}_3(\mathbf{t}), \\ d\mathcal{U}^L = [\tau\upsilon_3\mathcal{V}\mathcal{U}^A - (\sigma+\varsigma)\mathcal{U}^L]d\mathbf{t} + \wp_4\mathcal{U}^L d\mathcal{Q}_4(\mathbf{t}), \ if\ \mathsf{T}_2 \le \mathbf{t} \le \mathsf{T}, \\ d\mathcal{U}^A = [\sigma\mathcal{U}^L - \phi\mathcal{U}^A]d\mathbf{t} + \wp_7\mathcal{U}^A d\mathcal{Q}_7(\mathbf{t}), \\ d\mathcal{T} = [\omega_1\mathcal{G}^A - \rho\mathcal{T} - \omega_2\mathcal{Q}\mathcal{T}]d\mathbf{t} + \wp_6\mathcal{T}d\mathcal{Q}_6(\mathbf{t}), \\ d\mathcal{Q} = [\delta\mathcal{Q}\mathcal{T} - \varkappa\mathcal{Q}]d\mathbf{t} + \wp_7\mathcal{Q}d\mathcal{Q}_7(\mathbf{t}). \end{cases} \tag{3.3}$$

Here, we apply the technique described in [30] in the frame of Caputo's derivative to numerically review the piecewise structures (3.1)–(3.3). We set out the process by performing the following:

$$\begin{cases} \frac{d\Upsilon_{\mathbb{k}}(\mathbf{t})}{d\mathbf{t}} = F(\mathbf{t}, \Upsilon_{\mathbb{k}}).\ \Upsilon_{\mathbb{k}}(0) = \Upsilon_{\mathbb{k},0},\ \mathbb{k} = 1, 2, ..., \mathfrak{n}\ if\ \mathbf{t} \in [0, \mathsf{T}_1], \\ {}_{\mathsf{T}_1}^c\mathbf{D}_{\mathbf{t}}^{\eta}\Upsilon_{\mathbb{k}}(\mathbf{t}) = F(\mathbf{t}, \Upsilon_{\mathbb{k}}),\ \Upsilon_{\mathbb{k}}(\mathsf{T}_1) = \Upsilon_{\mathbb{k},1},\ if\ \mathbf{t} \in [\mathsf{T}_1, \mathsf{T}_2], \\ d\Upsilon_{\mathbb{k}}(\mathbf{t}) = F(\mathbf{t}, \Upsilon_{\mathbb{k}})d\mathbf{t} + \wp_{\mathbb{k}}\Upsilon_{\mathbb{k}}d\mathcal{Q}_{\mathbb{k}}(\mathbf{t}),\ \Upsilon_{\mathbb{k}}(\mathsf{T}_2) = \Upsilon_{\mathbb{k},2},\ if\ \mathbf{t} \in [\mathsf{T}_2, \mathsf{T}]. \end{cases}$$

It follows that

$$\Upsilon_{\mathbb{k}}^{\mathbf{v}} = \begin{cases} \Upsilon_{\mathbb{k}}(0) + \sum\limits_{J=2}^{\mathbf{v}} \Big\{ \frac{23}{12} F(\mathbf{t}_J, \Upsilon^J)\Delta\mathbf{t} - \frac{4}{3} F(\mathbf{t}_{J-1}, \Upsilon^{J-1})\Delta\mathbf{t} + \frac{7}{12} F(\mathbf{t}_{J-2}, \Upsilon^{J-2})\Delta\mathbf{t} \Big\}, \quad \mathbf{t} \in [0, \mathbf{T_1}]. \\ \Upsilon_{\mathbb{k}}(\mathsf{T}_1) + \frac{(\Delta\mathbf{t})^{\eta-1}}{\Gamma(\eta+1)} \sum\limits_{J=2}^{\mathbf{v}} F(\mathbf{t}_{J-2}, \Upsilon^{J-2})\mathfrak{I}_1 \\ \quad + \frac{(\Delta\mathbf{t})^{\eta-1}}{\Gamma(\eta+2)} \sum\limits_{J=2}^{\mathbf{v}} \Big\{ F(\mathbf{t}_{J-1}, \Upsilon^{J-1}) - F(\mathbf{t}_{J-2}, \Upsilon^{J-2}) \Big\}\mathfrak{I}_2 \\ \quad + \frac{\eta(\Delta\mathbf{t})^{\eta-1}}{2\Gamma(\eta+3)} \sum\limits_{J=2}^{\mathbf{v}} \Big\{ F(\mathbf{t}_J, \Upsilon^J) - 2F(\mathbf{t}_{J-1}, \Upsilon^{J-1}) + F(\mathbf{t}_{J-2}, \Upsilon^{J-2}) \Big\}\mathfrak{I}_3, \quad \mathbf{t} \in [\mathsf{T}_1, \mathsf{T}_2], \\ \Upsilon_{\mathbb{k}}(\mathsf{T}_2) + \sum\limits_{J=\mathbf{v}+3}^{\mathrm{n}} \Big\{ \frac{7}{12} F(\mathbf{t}_{J-2}, \Upsilon^{J-2})\Delta\mathbf{t} - \frac{4}{3} F(\mathbf{t}_{J-1}, \Upsilon^{J-1})\Delta\mathbf{t} + \frac{23}{12} F(\mathbf{t}_J, \Upsilon^J)\Delta\mathbf{t} \Big\} \\ \quad + \sum\limits_{J=\mathbf{v}+3}^{\mathrm{n}} \Big\{ \frac{7}{12}(B(\mathbf{t}_{J-1}) - B(\mathbf{t}_{J-2}))\wp\Upsilon^{J-2} - \frac{4}{3}(B(\mathbf{t}_J) - B(\mathbf{t}_{J-1}))\wp\Upsilon^{J-1} \\ \quad + \frac{23}{12}(B(\mathbf{t}_{J+1}) - B(\mathbf{t}_J))\wp\Upsilon^J \Big\}, \quad \mathbf{t} \in [\mathsf{T}_2, \mathsf{T}], \end{cases}$$

where

$$\mathfrak{I}_1 := (\mathbf{v} - J - 1)^{\eta} - (\mathbf{v} - J)^{\eta}, \tag{3.4}$$

$$\mathfrak{I}_2 := (\mathbf{v} - J + 1)^{\eta}(\mathbf{v} - J + 2\eta + 3) - (\mathbf{v} - J)^{\eta}(\mathbf{v} - J + 3\eta + 3), \tag{3.5}$$

and

$$\mathfrak{I}_3 := \begin{cases} (\mathbf{v} - J + 1)^{\eta}\Big(2(\mathbf{v} - J)^2 + (3\eta + 10)(\mathbf{v} - J) + 2\eta^2 + 9\eta + 12\Big), \\ \quad + (\mathbf{v} - J)^{\eta}\Big(2(\mathbf{v} - J)^2 + (5\eta + 10)(\mathbf{v} - J) + 6\eta^2 + 18\eta + 12\Big). \end{cases} \tag{3.6}$$

3.2. Proposed model via exponential decay kernel

In what follows, we aim to investigate the codynamics of the HIV-1/HTLV-I models (2.1) and (2.3) that include responses of immunity and cellular outbreak, including integer-order, exponential decay and culminating in the random procedures. If T is identified as the last phase of dissemination, then the conceptual structure will be constructed in the initial stage employing the integer-order derivative form, followed by the exponential decay kernel in the next phase, culminating in the random setting in the following steps. Following that, a numerical convention that clarifies this occurrence is offered as:

$$\begin{cases} \frac{d\mathcal{V}}{d\mathbf{t}} = \vartheta - \beta\mathcal{V} - \upsilon_1\mathcal{V}\mathcal{T} - \upsilon_2\mathcal{V}\mathcal{G}^A - \upsilon_3\mathcal{V}\mathcal{U}^A, \\ \frac{d\mathcal{G}^L}{d\mathbf{t}} = (1 - \lambda)(\upsilon_1\mathcal{V}\mathcal{T} + \upsilon_2\mathcal{V}\mathcal{G}^A) - (\epsilon + \xi)\mathcal{G}^L, \\ \frac{d\mathcal{G}^L}{d\mathbf{t}} = \lambda(\upsilon_1\mathcal{V}\mathcal{T} + \upsilon_2\mathcal{V}\mathcal{G}^A) + \epsilon\mathcal{G}^L - \varrho\mathcal{G}^A, \\ \frac{d\mathcal{U}^L}{d\mathbf{t}} = \tau\upsilon_3\mathcal{V}\mathcal{U}^A - (\sigma + \varsigma)\mathcal{U}^L, \ if\ 0 \le \mathbf{t} \le \mathsf{T}_1, \\ \frac{d\mathcal{U}^A}{d\mathbf{t}} = \sigma\mathcal{U}^L - \phi\mathcal{U}^A, \\ \frac{d\mathcal{T}}{d\mathbf{t}} = \omega_1\mathcal{G}^A - \rho\mathcal{T} - \omega_2\mathcal{Q}\mathcal{T}, \\ \frac{d\mathcal{Q}}{d\mathbf{t}} = \delta\mathcal{Q}\mathcal{T} - \varkappa\mathcal{Q}. \end{cases} \tag{3.7}$$

$$\begin{cases} {}^{CF}_{0}\mathbf{D}^{\eta}_{\mathbf{t}}\mathcal{V} = \vartheta - \beta\mathcal{V} - \upsilon_1\mathcal{V}\mathcal{T} - \upsilon_2\mathcal{V}\mathcal{G}^A - \upsilon_3\mathcal{V}\mathcal{U}^A, \\ {}^{CF}_{0}\mathbf{D}^{\eta}_{\mathbf{t}}\mathcal{G}^L = (1-\lambda)(\upsilon_1\mathcal{V}\mathcal{T} + \upsilon_2\mathcal{V}\mathcal{G}^A) - (\epsilon+\xi)\mathcal{G}^L, \\ {}^{CF}_{0}\mathbf{D}^{\eta}_{\mathbf{t}}\mathcal{G}^L = \lambda(\upsilon_1\mathcal{V}\mathcal{T} + \upsilon_2\mathcal{V}\mathcal{G}^A) + \epsilon\mathcal{G}^L - \varrho\mathcal{G}^A, \\ {}^{CF}_{0}\mathbf{D}^{\eta}_{\mathbf{t}}\mathcal{U}^L = \tau\upsilon_3\mathcal{V}\mathcal{U}^A - (\sigma+\varsigma)\mathcal{U}^L, \ if \ \mathsf{T}1 \le \mathbf{t} \le \mathsf{T}2, \\ {}^{CF}_{0}\mathbf{D}^{\eta}_{\mathbf{t}}\mathcal{U}^A = \sigma\mathcal{U}^L - \phi\mathcal{U}^A, \\ {}^{CF}_{0}\mathbf{D}^{\eta}_{\mathbf{t}}\mathcal{T} = \omega_1\mathcal{G}^A - \rho\mathcal{T} - \omega_2\mathcal{Q}\mathcal{T}, \\ {}^{CF}_{0}\mathbf{D}^{\eta}_{\mathbf{t}}\mathcal{Q} = \delta\mathcal{Q}\mathcal{T} - \varkappa\mathcal{Q}. \end{cases} \tag{3.8}$$

$$\begin{cases} d\mathcal{V} = [\vartheta - \beta\mathcal{V} - \upsilon_1\mathcal{V}\mathcal{T} - \upsilon_2\mathcal{V}\mathcal{G}^A - \upsilon_3\mathcal{V}\mathcal{U}^A] + \wp_1\mathcal{V}d\mathcal{Q}_1(\mathbf{t}), \\ d\mathcal{G}^L = [(1-\lambda)(\upsilon_1\mathcal{V}\mathcal{T} + \upsilon_2\mathcal{V}\mathcal{G}^A) - (\epsilon+\xi)\mathcal{G}^L] + \wp_2\mathcal{G}^L d\mathcal{Q}_2(\mathbf{t}), \\ d\mathcal{G}^A = [\lambda(\upsilon_1\mathcal{V}\mathcal{T} + \upsilon_2\mathcal{V}\mathcal{G}^A) + \epsilon\mathcal{G}^L - \varrho\mathcal{G}^A] + \wp_3\mathcal{G}^A d\mathcal{Q}_3(\mathbf{t}), \\ d\mathcal{U}^L = [\tau\upsilon_3\mathcal{V}\mathcal{U}^A - (\sigma+\varsigma)\mathcal{U}^L] + \wp_4\mathcal{U}^L d\mathcal{Q}_4(\mathbf{t}), \ if \ \mathsf{T}2 \le \mathbf{t} \le \mathsf{T}, \\ d\mathcal{U}^A = [\sigma\mathcal{U}^L - \phi\mathcal{U}^A] + \wp_7\mathcal{U}^A d\mathcal{Q}_7(\mathbf{t})] + \wp_7\mathcal{U}^A d\mathcal{Q}_7(\mathbf{t}), \\ d\mathcal{T} = [\omega_1\mathcal{G}^A - \rho\mathcal{T} - \omega_2\mathcal{Q}\mathcal{T}] + \wp_6\mathcal{T}d\mathcal{Q}_6(\mathbf{t}), \\ d\mathcal{Q} = [\delta\mathcal{Q}\mathcal{T} - \varkappa\mathcal{Q}] + \wp_7\mathcal{Q}d\mathcal{Q}_7(\mathbf{t}). \end{cases} \tag{3.9}$$

Here, we apply the technique described in [30] in the frame of Caputo-Fabrizio derivative to numerically review the piecewise structures (3.7)–(3.9). We set out the process by performing the following:

$$\begin{cases} \frac{d\Upsilon_{\mathbb{k}}(\mathbf{t})}{d\mathbf{t}} = F(\mathbf{t}, \Upsilon_{\mathbb{k}}). \ \Upsilon_{\mathbb{k}}(0) = \Upsilon_{\mathbb{k},0}, \ \mathbb{k} = 1, 2, ..., \mathfrak{n} \ if \ \mathbf{t} \in [0, \mathsf{T}_1], \\ {}^{CF}_{\mathsf{T}1}\mathbf{D}^{\eta}_{\mathbf{t}}\Upsilon_{\mathbb{k}}(\mathbf{t}) = F(\mathbf{t}, \Upsilon_{\mathbb{k}}), \ \Upsilon_{\mathbb{k}}(\mathsf{T}_1) = \Upsilon_{\mathbb{k},1}, \ if \ \mathbf{t} \in [\mathsf{T}_1, \mathsf{T}_2], \\ d\Upsilon_{\mathbb{k}}(\mathbf{t}) = F(\mathbf{t}, \Upsilon_{\mathbb{k}})d\mathbf{t} + \wp_{\mathbb{k}}\Upsilon_{\mathbb{k}}d\mathcal{Q}_{\mathbb{k}}(\mathbf{t}), \ \Upsilon_{\mathbb{k}}(\mathsf{T}_2) = \Upsilon_{\mathbb{k},2}, \ if \ \mathbf{t} \in [\mathsf{T}_2, \mathsf{T}]. \end{cases} \tag{3.10}$$

It follows that

$$\Upsilon^{\mathbf{v}}_{\mathbb{k}} = \begin{cases} \Upsilon_{\mathbb{k}}(0) + \sum\limits_{J=2}^{\mathbf{v}} \left\{ \frac{23}{12}F(\mathbf{t}_J, \Upsilon^J)\Delta\mathbf{t} - \frac{4}{3}F(\mathbf{t}_{J-1}, \Upsilon^{J-1})\Delta\mathbf{t} + \frac{7}{12}F(\mathbf{t}_{J-2}, \Upsilon^{J-2})\Delta\mathbf{t} \right\}, \ \ \mathbf{t} \in [0, \mathbf{T_1}]. \\ \Upsilon_{\mathbb{k}}(\mathsf{T}_1) + \frac{1-\eta}{\mathbb{M}(\eta)}F(\mathbf{t}_{\mathfrak{n}}, \Upsilon^{\mathfrak{n}}) + \frac{\eta}{\mathbb{M}(\eta)} \sum\limits_{J=2}^{\mathbf{v}} \left\{ \frac{7}{12}F(\mathbf{t}_{J-2}, \Upsilon^{J-2})\Delta\mathbf{t} - \frac{4}{3}F(\mathbf{t}_{J-1}, \Upsilon^{J-1})\Delta\mathbf{t} \right. \\ \quad \left. + \frac{23}{12}F(\mathbf{t}_J, \Upsilon^J)\Delta\mathbf{t} \right\}, \ \ \mathbf{t} \in [\mathsf{T}_1, \mathsf{T}_2], \\ \Upsilon_{\mathbb{k}}(\mathsf{T}_2) + \sum\limits_{J=\mathbf{v}+3}^{\mathfrak{n}} \left\{ \frac{7}{12}F(\mathbf{t}_{J-2}, \Upsilon^{J-2})\Delta\mathbf{t} - \frac{4}{3}F(\mathbf{t}_{J-1}, \Upsilon^{J-1})\Delta\mathbf{t} + \frac{23}{12}F(\mathbf{t}_J, \Upsilon^J)\Delta\mathbf{t} \right\} \\ \quad + \sum\limits_{J=\mathbf{v}+3}^{\mathfrak{n}} \left\{ \frac{7}{12}(B(\mathbf{t}_{J-1}) - B(\mathbf{t}_{J-2}))\wp\Upsilon^{J-2} - \frac{4}{3}(B(\mathbf{t}_J) - B(\mathbf{t}_{J-1}))\wp\Upsilon^{J-1} \right. \\ \quad \left. + \frac{23}{12}(B(\mathbf{t}_{J+1}) - B(\mathbf{t}_J))\wp\Upsilon^J \right\}, \ \ \mathbf{t} \in [\mathsf{T}_2, \mathsf{T}]. \end{cases} \tag{3.11}$$

3.3. Proposed scheme via generalized Mittag-Leffler kernel

This section devotes to investigate the codynamics of the HIV-1/HTLV-I models (2.1) and (2.3) that include responses of immunity and cellular outbreak, including integer-order, generalized

Mittag-Leffler kernel and culminating in the random procedures. If T is identified as the last phase of dissemination, then the conceptual structure will be constructed in the initial stage employing the integer-order derivative form, followed by the generalized Mittag-Leffler kernel in the next phase, culminating in the random setting in the following steps. Following that, a numerical convention that clarifies this occurrence is offered as:

$$\begin{cases} \frac{d\mathcal{V}}{d\mathbf{t}} = \vartheta - \beta\mathcal{V} - \upsilon_1\mathcal{V}\mathcal{T} - \upsilon_2\mathcal{V}\mathcal{G}^A - \upsilon_3\mathcal{V}\mathcal{U}^A, \\ \frac{d\mathcal{G}^L}{d\mathbf{t}} = (1-\lambda)(\upsilon_1\mathcal{V}\mathcal{T} + \upsilon_2\mathcal{V}\mathcal{G}^A) - (\epsilon+\xi)\mathcal{G}^L, \\ \frac{d\mathcal{G}^L}{d\mathbf{t}} = \lambda(\upsilon_1\mathcal{V}\mathcal{T} + \upsilon_2\mathcal{V}\mathcal{G}^A) + \epsilon\mathcal{G}^L - \varrho\mathcal{G}^A, \\ \frac{d\mathcal{U}^L}{d\mathbf{t}} = \tau\upsilon_3\mathcal{V}\mathcal{U}^A - (\sigma+\varsigma)\mathcal{U}^L, \ if\ 0 \le \mathbf{t} \le \mathsf{T}1, \\ \frac{d\mathcal{U}^A}{d\mathbf{t}} = \sigma\mathcal{U}^L - \phi\mathcal{U}^A, \\ \frac{d\mathcal{T}}{d\mathbf{t}} = \omega_1\mathcal{G}^A - \rho\mathcal{T} - \omega_2\mathcal{Q}\mathcal{T}, \\ \frac{dQ}{d\mathbf{t}} = \delta\mathcal{Q}\mathcal{T} - \varkappa\mathcal{Q}. \end{cases} \tag{3.12}$$

$$\begin{cases} {}^{ABC}_{0}\mathbf{D}^{\eta}_{\mathbf{t}}\mathcal{V} = \vartheta - \beta\mathcal{V} - \upsilon_1\mathcal{V}\mathcal{T} - \upsilon_2\mathcal{V}\mathcal{G}^A - \upsilon_3\mathcal{V}\mathcal{U}^A, \\ {}^{ABC}_{0}\mathbf{D}^{\eta}_{\mathbf{t}}\mathcal{G}^L = (1-\lambda)(\upsilon_1\mathcal{V}\mathcal{T} + \upsilon_2\mathcal{V}\mathcal{G}^A) - (\epsilon+\xi)\mathcal{G}^L, \\ {}^{ABC}_{0}\mathbf{D}^{\eta}_{\mathbf{t}}\mathcal{G}^L = \lambda(\upsilon_1\mathcal{V}\mathcal{T} + \upsilon_2\mathcal{V}\mathcal{G}^A) + \epsilon\mathcal{G}^L - \varrho\mathcal{G}^A, \\ {}^{ABC}_{0}\mathbf{D}^{\eta}_{\mathbf{t}}\mathcal{U}^L = \tau\upsilon_3\mathcal{V}\mathcal{U}^A - (\sigma+\varsigma)\mathcal{U}^L, \ if\ \mathsf{T}1 \le \mathbf{t} \le \mathsf{T}2, \\ {}^{ABC}_{0}\mathbf{D}^{\eta}_{\mathbf{t}}\mathcal{U}^A = \sigma\mathcal{U}^L - \phi\mathcal{U}^A, \\ {}^{ABC}_{0}\mathbf{D}^{\eta}_{\mathbf{t}}\mathcal{T} = \omega_1\mathcal{G}^A - \rho\mathcal{T} - \omega_2\mathcal{Q}\mathcal{T}, \\ {}^{ABC}_{0}\mathbf{D}^{\eta}_{\mathbf{t}}\mathcal{Q} = \delta\mathcal{Q}\mathcal{T} - \varkappa\mathcal{Q}. \end{cases} \tag{3.13}$$

$$\begin{cases} d\mathcal{V} = [\vartheta - \beta\mathcal{V} - \upsilon_1\mathcal{V}\mathcal{T} - \upsilon_2\mathcal{V}\mathcal{G}^A - \upsilon_3\mathcal{V}\mathcal{U}^A] + \wp_1\mathcal{V}d\mathcal{Q}_1(\mathbf{t}), \\ d\mathcal{G}^L = [(1-\lambda)(\upsilon_1\mathcal{V}\mathcal{T} + \upsilon_2\mathcal{V}\mathcal{G}^A) - (\epsilon+\xi)\mathcal{G}^L] + \wp_2\mathcal{G}^L d\mathcal{Q}_2(\mathbf{t}), \\ d\mathcal{G}^A = [\lambda(\upsilon_1\mathcal{V}\mathcal{T} + \upsilon_2\mathcal{V}\mathcal{G}^A) + \epsilon\mathcal{G}^L - \varrho\mathcal{G}^A] + \wp_3\mathcal{G}^A d\mathcal{Q}_3(\mathbf{t}), \\ d\mathcal{U}^L = [\tau\upsilon_3\mathcal{V}\mathcal{U}^A - (\sigma+\varsigma)\mathcal{U}^L] + \wp_4\mathcal{U}^L d\mathcal{Q}_4(\mathbf{t}), \ if\ \mathsf{T}2 \le \mathbf{t} \le \mathsf{T}, \\ d\mathcal{U}^A = [\sigma\mathcal{U}^L - \phi\mathcal{U}^A] + \wp_7\mathcal{U}^A d\mathcal{Q}_7(\mathbf{t})] + \wp_7\mathcal{U}^A d\mathcal{Q}_7(\mathbf{t}), \\ d\mathcal{T} = [\omega_1\mathcal{G}^A - \rho\mathcal{T} - \omega_2\mathcal{Q}\mathcal{T}] + \wp_6\mathcal{T}d\mathcal{Q}_6(\mathbf{t}), \\ d\mathcal{Q} = [\delta\mathcal{Q}\mathcal{T} - \varkappa\mathcal{Q}] + \wp_7\mathcal{Q}d\mathcal{Q}_7(\mathbf{t}). \end{cases} \tag{3.14}$$

Here, we apply the technique described in [30] in the frame of Atanagan-Baleanu-Caputo derivative to numerically review the piecewise structures (3.12)–(3.14). We set out the process by performing the following:

$$\begin{cases} \frac{d\Upsilon_{\mathbb{k}}(\mathbf{t})}{d\mathbf{t}} = F(\mathbf{t}, \Upsilon_{\mathbb{k}}).\ \Upsilon_{\mathbb{k}}(0) = \Upsilon_{\mathbb{k},0},\ \mathbb{k} = 1, 2, ..., \mathfrak{n}\ if\ \mathbf{t} \in [0, \mathsf{T}1], \\ {}^{ABC}_{\mathsf{T}1}\mathbf{D}^{\eta}_{\mathbf{t}}\Upsilon_{\mathbb{k}}(\mathbf{t}) = F(\mathbf{t}, \Upsilon_{\mathbb{k}}),\ \Upsilon_{\mathbb{k}}(\mathsf{T}1) = \Upsilon_{\mathbb{k},1},\ if\ \mathbf{t} \in [\mathsf{T}1, \mathsf{T}2], \\ d\Upsilon_{\mathbb{k}}(\mathbf{t}) = F(\mathbf{t}, \Upsilon_{\mathbb{k}})d\mathbf{t} + \wp_{\mathbb{k}}\Upsilon_{\mathbb{k}}d\mathcal{Q}_{\mathbb{k}}(\mathbf{t}),\ \Upsilon_{\mathbb{k}}(\mathsf{T}2) = \Upsilon_{\mathbb{k},2},\ if\ \mathbf{t} \in [\mathsf{T}2, \mathsf{T}]. \end{cases}$$

It follows that

$$\Upsilon_{\mathbb{k}}^{\mathbf{v}} = \begin{cases} \Upsilon_{\mathbb{k}}(0) + \sum\limits_{J=2}^{\mathbf{v}} \Big\{ \frac{23}{12} F(\mathbf{t}_J, \Upsilon^J)\Delta\mathbf{t} - \frac{4}{3} F(\mathbf{t}_{J-1}, \Upsilon^{J-1})\Delta\mathbf{t} + \frac{7}{12} F(\mathbf{t}_{J-2}, \Upsilon^{J-2})\Delta\mathbf{t} \Big\}, \quad \mathbf{t} \in [0, \mathbf{T_1}]. \\ \Upsilon_{\mathbb{k}}(\mathsf{T}_1) + \frac{\eta}{ABC(\eta)} F(\mathbf{t}_{\mathrm{n}}, \Upsilon^{\mathrm{n}}) + \frac{\eta(\Delta\mathbf{t})^{\eta-1}}{ABC(\eta)\Gamma(\eta+1)} \sum\limits_{J=2}^{\mathbf{v}} F(\mathbf{t}_{J-2}, \Upsilon^{J-2})\mathfrak{I}_1 \\ \quad + \frac{\eta(\Delta\mathbf{t})^{\eta-1}}{ABC(\eta)\Gamma(\eta+2)} \sum\limits_{J=2}^{\mathbf{v}} \Big\{ F(\mathbf{t}_{J-1}, \Upsilon^{J-1}) - F(\mathbf{t}_{J-2}, \Upsilon^{J-2}) \Big\}\mathfrak{I}_2 \\ \quad + \frac{\eta(\Delta\mathbf{t})^{\eta-1}}{2ABC(\eta)\Gamma(\eta+3)} \sum\limits_{J=2}^{\mathbf{v}} \Big\{ F(\mathbf{t}_J, \Upsilon^J) - 2F(\mathbf{t}_{J-1}, \Upsilon^{J-1}) + F(\mathbf{t}_{J-2}, \Upsilon^{J-2}) \Big\}\mathfrak{I}_3, \quad \mathbf{t} \in [\mathsf{T}_1, \mathsf{T}_2], \\ \Upsilon_{\mathbb{k}}(\mathsf{T}_2) + \sum\limits_{J=\mathbf{v}+3}^{\mathrm{n}} \Big\{ \frac{7}{12} F(\mathbf{t}_{J-2}, \Upsilon^{J-2})\Delta\mathbf{t} - \frac{4}{3} F(\mathbf{t}_{J-1}, \Upsilon^{J-1})\Delta\mathbf{t} + \frac{23}{12} F(\mathbf{t}_J, \Upsilon^J)\Delta\mathbf{t} \Big\} \\ \quad + \sum\limits_{J=\mathbf{v}+3}^{\mathrm{n}} \Big\{ \frac{7}{12} (B(\mathbf{t}_{J-1}) - B(\mathbf{t}_{J-2}))\wp\Upsilon^{J-2} - \frac{4}{3} (B(\mathbf{t}_J) - B(\mathbf{t}_{J-1}))\wp\Upsilon^{J-1} \\ \quad + \frac{23}{12} (B(\mathbf{t}_{J+1}) - B(\mathbf{t}_J))\wp\Upsilon^J \Big\}, \quad \mathbf{t} \in [\mathsf{T}_2, \mathsf{T}], \end{cases}$$

where $\mathfrak{I}_1, \mathfrak{I}_2$ and $\mathfrak{I}_3$ are stated before in (3.4)–(3.6).

3.4. Experimental consequences

In this section, we will show numerical modelling concepts that use the Atangana and Araz methods referenced previously [30] to substantiate research hypotheses. Multiple numerical illustrations are used to exemplify the suitability and utility of the proposed HIV-1/HTLV-I structure in the deterministic-stochastic setting. All figurative and numerical calculations were carried out using the MATLAB 21 software.

Table 2. Some configurations of biological process variables (2.3) from Table 1.

Combinations	Values
$(\mathcal{A}_1)$	$\upsilon_1 = \upsilon_2 = \upsilon_3 = 0.0001,\ \delta = 0.01,\ \wp_1 = 0.01, \wp_2 = 0.012,$ $\wp_3 = 0.02, \wp_4 = 0.03,\ \wp_5 = 0.04,\ \wp_6 = 0.05,\ \wp_7 = 0.06.$
$(\mathcal{A}_2)$	$\upsilon_1 = \upsilon_2 = \upsilon_3 = 0.0003,\ \delta = 0.001,\ \wp_1 = 0.01, \wp_2 = 0.012,$ $\wp_3 = 0.02, \wp_4 = 0.03,\ \wp_5 = 0.04,\ \wp_6 = 0.05,\ \wp_7 = 0.06.$
$(\mathcal{A}_3)$	$\upsilon_1 = \upsilon_2 = 0.0001,\ \upsilon_3 = 0.003,\ \delta = 0.001,\ \wp_1 = 0.01, \wp_2 = 0.012,$ $\wp_3 = 0.02, \wp_4 = 0.03,\ \wp_5 = 0.04,\ \wp_6 = 0.05,\ \wp_7 = 0.06.$
$(\mathcal{A}_4)$	$\upsilon_1 = \upsilon_2 = 0.0003,\ \upsilon_3 = 0.002,\ \delta = 0.01,\ \wp_1 = 0.01, \wp_2 = 0.012,$ $\wp_3 = 0.02, \wp_4 = 0.03,\ \wp_5 = 0.04,\ \wp_6 = 0.05,\ \wp_7 = 0.06.$
$(\mathcal{A}_5)$	$\upsilon_1 = \upsilon_2 = 0.0005,\ \upsilon_3 = 0.003,\ \delta = 0.1.$
$(\mathcal{A}_6)$	$\upsilon_1 = \upsilon_2 = 0.0005,\ \upsilon_3 = 0.003,\ \delta - -varied.$

We determine numerically the pathways for the stochastic ailment framework (3.1)–(3.2) and its commensurate deterministic structure to demonstrate our findings. The time interval is $[0, 100]$ units, while the initial values $(\mathcal{V}, \mathcal{G}^L, \mathcal{G}^A, \mathcal{U}^L, \mathcal{U}^A, \mathcal{T}, \mathcal{Q})(0) = (600, 0.5, 1.5, 1, 2, 5, 1)$. By Table 2, we re-select the amalgamation $(\mathcal{A}_1)$ as the valuation of the mechanism of biological parameters for (3.1)–(3.2) via piecewise technique. A straightforward computations demonstrates that

$\mathbb{R}_0^p = \frac{\vartheta\lambda\upsilon_2}{\beta(\varrho+\frac{\varphi_3^2}{2})} < 1$. According to Theorem 2.2, HIV-1/HTLV-I will become exterminated with unit probability, then become stable at fractional order $\eta = 0.95$. Moreover, when $\mathcal{R}_0 < 1$ (see [20]), the deterministic solution (3.1) under $(\mathcal{A}_1)$ and $(\mathcal{A}_2)$ suggests that both HIV-1 and HTLV-I are expected to die out, regardless of the ICs. Attempting to make (3.1)–(3.2) will be an appropriate strategy from a control standpoint, but HTLV-I and HIV-1 viruses are prolonged and the pathogens are very seldom removed. Figure 1 can illustrate the above two conclusions. Figures 2–4 shows the corresponding three ICs, $(\mathcal{V}, \mathcal{G}^L, \mathcal{G}^A, \mathcal{U}^L, \mathcal{U}^A, \mathcal{T}, \mathcal{Q})(0) = (400, 1, 1, 1.5, 4, 2, 2)$, $(\mathcal{V}, \mathcal{G}^L, \mathcal{G}^A, \mathcal{U}^L, \mathcal{U}^A, \mathcal{T}, \mathcal{Q})(0) = (200, 1.5, 0.5, 2, 6, 1.5, 3)$ and $(\mathcal{V}, \mathcal{G}^L, \mathcal{G}^A, \mathcal{U}^L, \mathcal{U}^A, \mathcal{T}, \mathcal{Q})(0) = (500, 3, 1.5, 0.8, 3, 2, 3)$, under varying population systems.

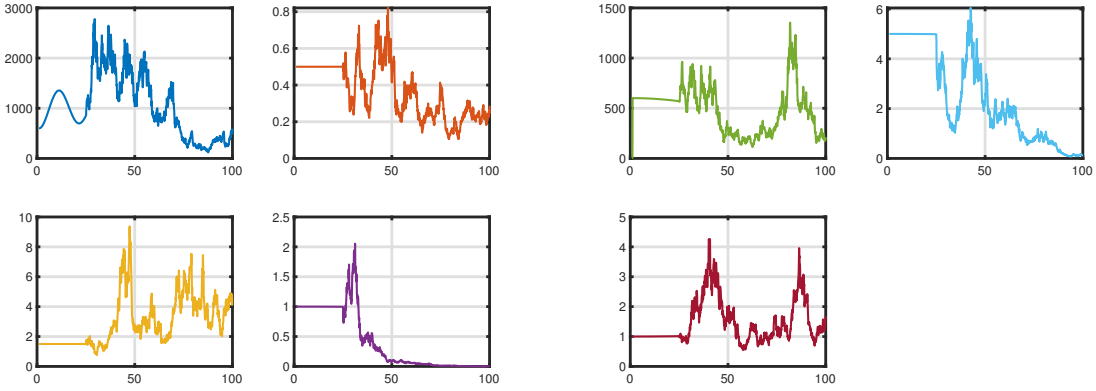

Figure 1. The HIV-1/HTLV-I model exhibits deterministic-stochastic behaviour with humoral immune response and cellular outbreak (3.1)–(3.3) via the power-law memory with $\eta = 0.95$ and white noises with ICs of $(600, 0.5, 1.5, 1, 2, 5, 1)$.

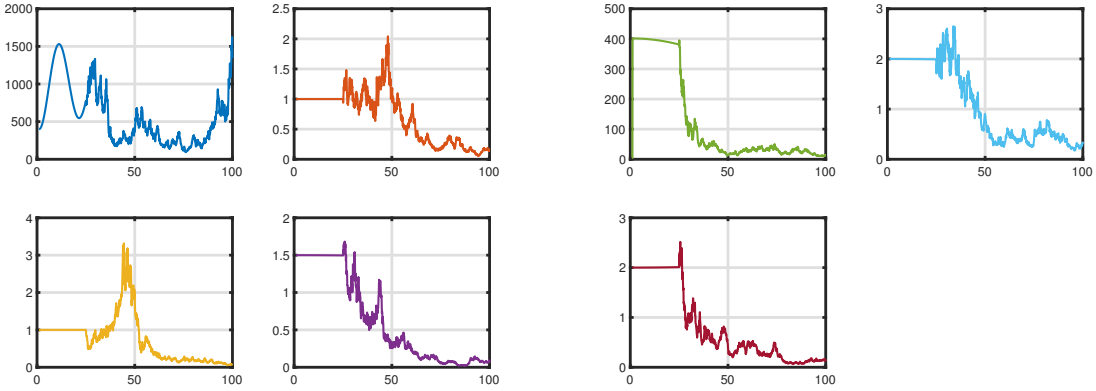

Figure 2. The HIV-1/HTLV-I model exhibits deterministic-stochastic behaviour with humoral immune response and cellular outbreak (3.1)–(3.3) via the power-law memory with $\eta = 0.95$ and white noises with ICs of $(400, 1, 1, 1.5, 4, 2, 2)$.

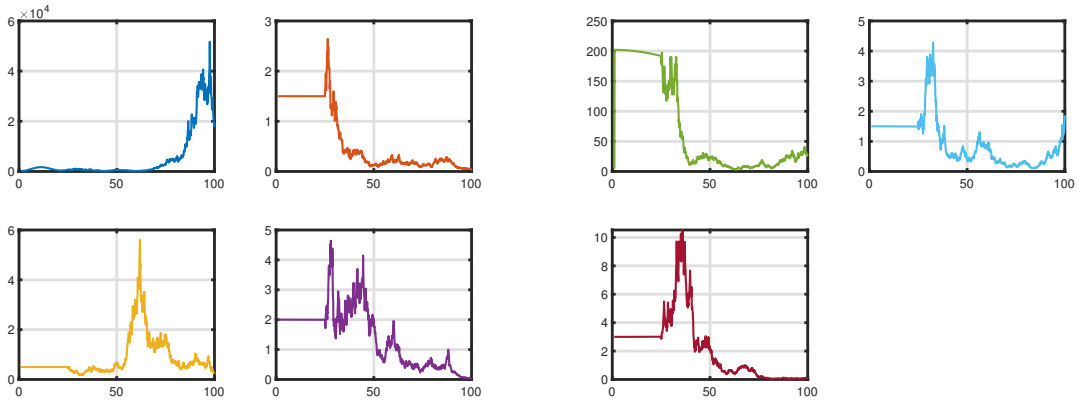

Figure 3. The HIV-1/HTLV-I model exhibits deterministic-stochastic behaviour with humoral immune response and cellular outbreak (3.1)–(3.3) via the power-law memory with $\eta = 0.95$ and white noises with ICs of $(200, 1.5, 0.5, 2, 6, 1.5, 3)$.

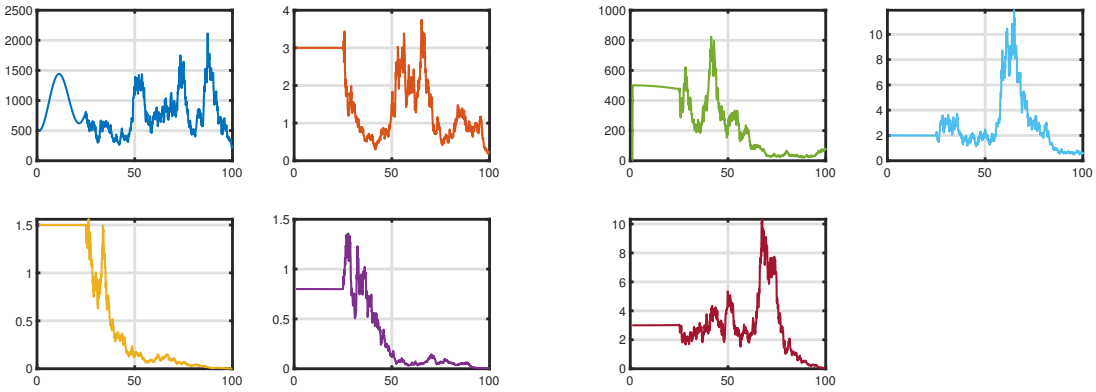

Figure 4. The HIV-1/HTLV-I model exhibits deterministic-stochastic behaviour with humoral immune response and cellular outbreak (3.1)–(3.3) via the power-law memory with $\eta = 0.95$ and white noises with ICs of $(500, 3, 1.5, 0.8, 3, 2, 3)$.

Applying the analogous technique to Caputo-Fabrizio system of DEs (3.7)–(3.9), we consider the same parameters as in $(\mathcal{A}_1)$ and $(\mathcal{A}_2)$, but alter the ICs as stated above. The threshold quantities $\mathcal{R}_0 > 1$ (see [20]) and $\mathbb{R}_0^s > 1$ can be easily calculated. The codynamics will proceed in the mean, as illustrated in Figure 5, assisting outcome of Theorem 2.3 (see Figures 6–8). This finding implies that HTLV-I will become extinct while HIV-1 will become systemic with unproductive humoral immunity.

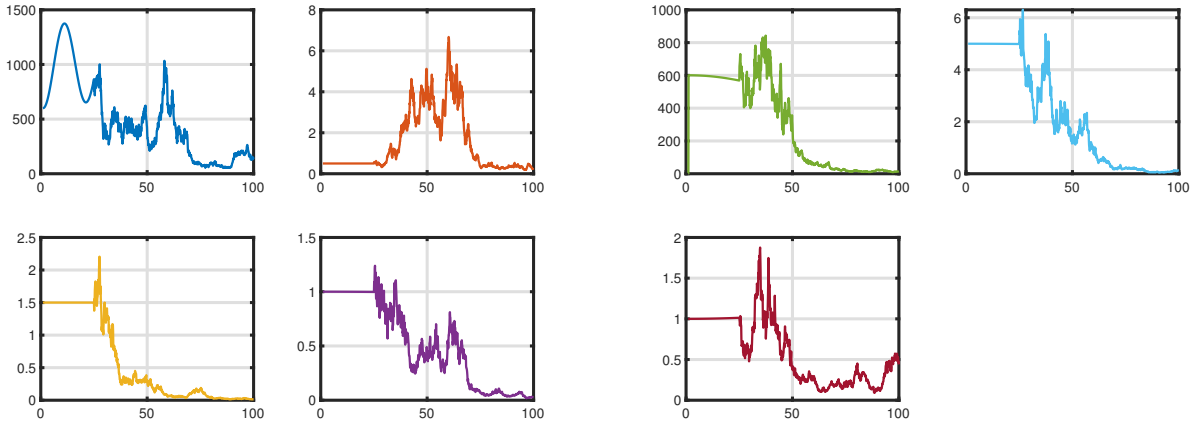

Figure 5. The HIV-1/HTLV-I model exhibits deterministic-stochastic behaviour with humoral immune response and cellular outbreak (3.7)–(3.9) via the exponential decay memory with $\eta = 0.95$ and white noises with ICs of $(600, 0.5, 1.5, 1, 2, 5, 1)$.

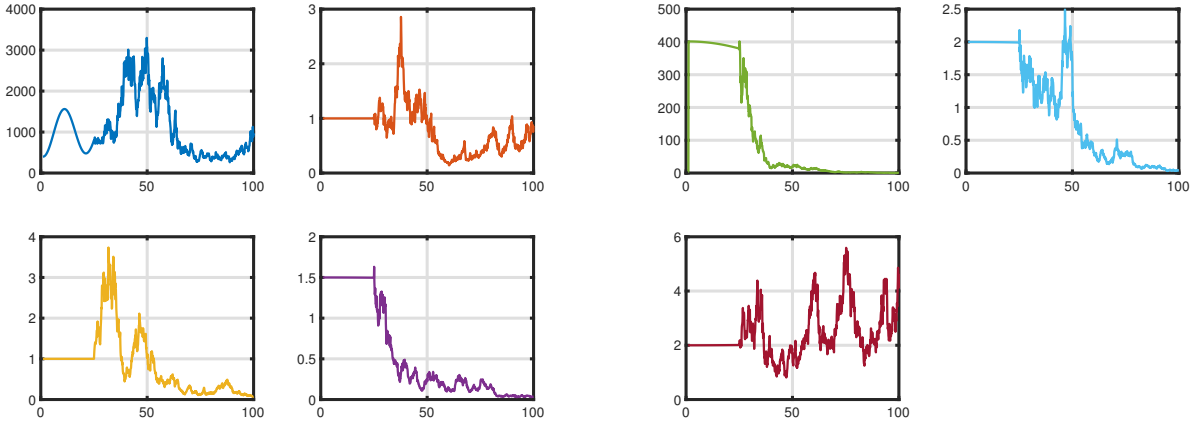

Figure 6. The HIV-1/HTLV-I model exhibits deterministic-stochastic behaviour with humoral immune response and cellular outbreak (3.7)–(3.9) via the exponential decay with $\eta = 0.95$ and white noises with ICs of $(400, 1, 1, 1.5, 4, 2, 2)$.

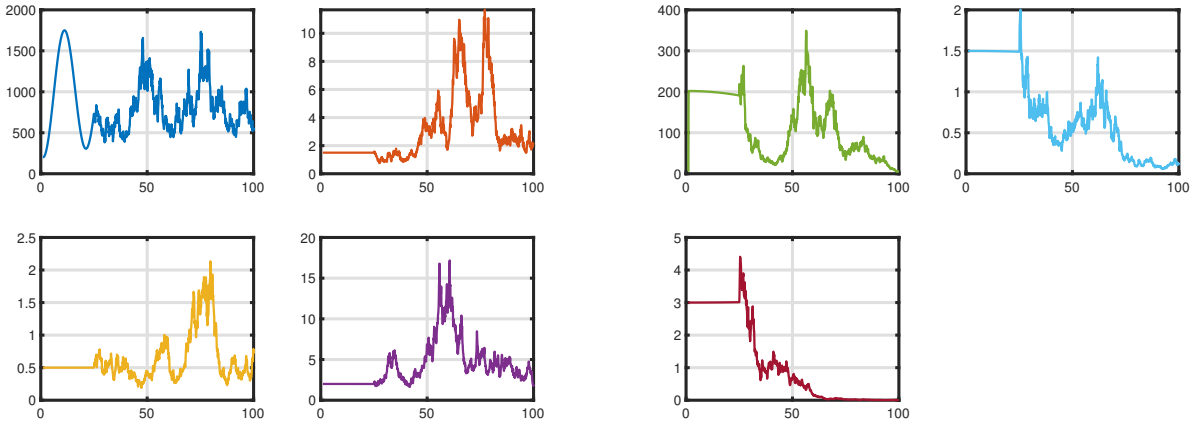

Figure 7. The HIV-1/HTLV-I model exhibits deterministic-stochastic behaviour with humoral immune response and cellular outbreak (3.7)–(3.9) via the exponential decay with $\eta = 0.95$ and white noises with ICs of $(200, 1.5, 0.5, 2, 6, 1.5, 3)$.

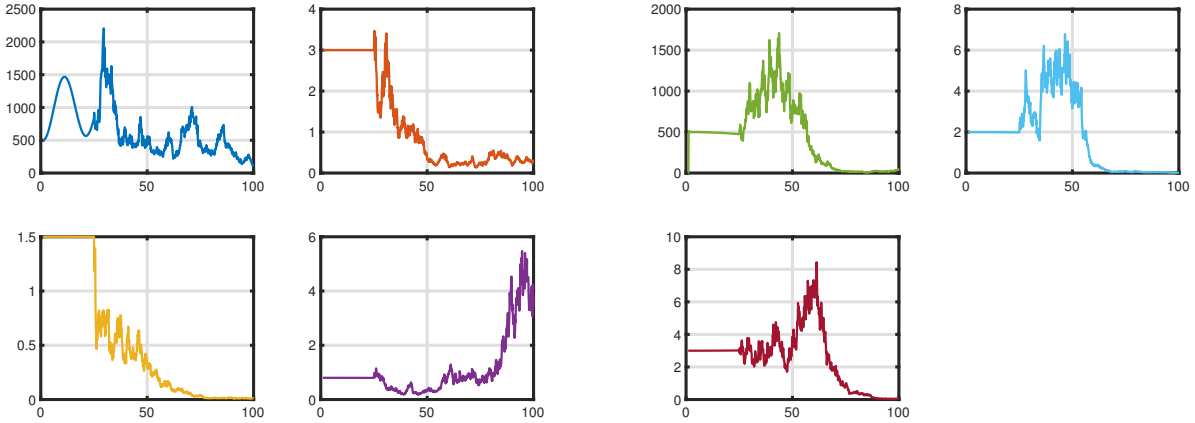

Figure 8. The HIV-1/HTLV-I model exhibits deterministic-stochastic behaviour with humoral immune response and cellular outbreak (3.7)–(3.9) via the exponential decay memory with $\eta = 0.95$ and white noises with ICs of $(500, 3, 1.5, 0.8, 3, 2, 3)$.

Considering the environmental intensities and parametric variations mentioned in $(\mathcal{A}_3)$ and $(\mathcal{A}_4)$, the numerical results for (3.12)–(3.14) will be an appropriate strategy from a control standpoint. Theorems 2.2 and 2.3 illustrate that there exists an ESD of probabilistic model (2.3). These findings indicate that HIV-1 will become extinct, whereas HTLV-I will become persistent. This is supported by the Figures 9–12.

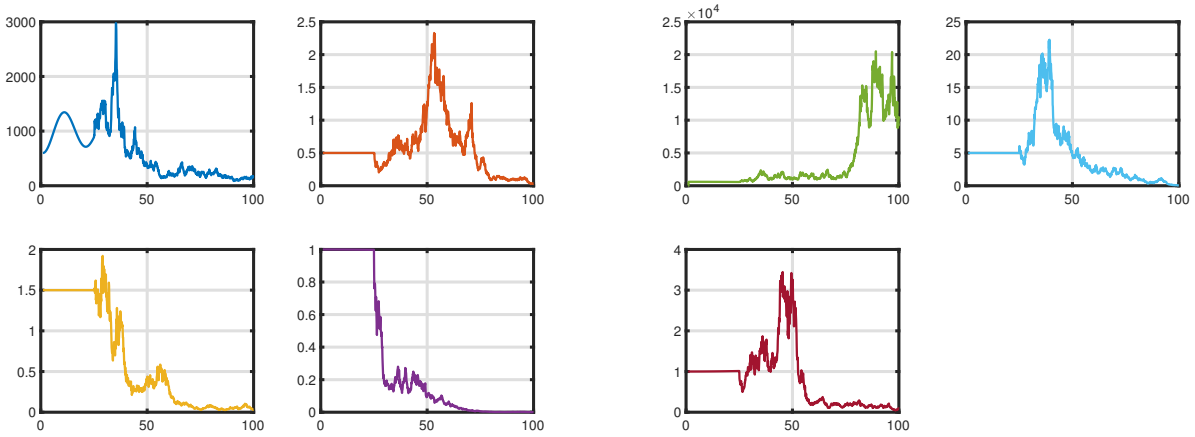

(a) **(b)**

Figure 9. The HIV-1/HTLV-I model exhibits deterministic-stochastic behaviour with humoral immune response and cellular outbreak (3.12)–(3.14) via the generalized Mittag-Leffler kernel with $\eta = 0.95$ and white noises with ICs of $(600, 0.5, 1.5, 1, 2, 5, 1)$.

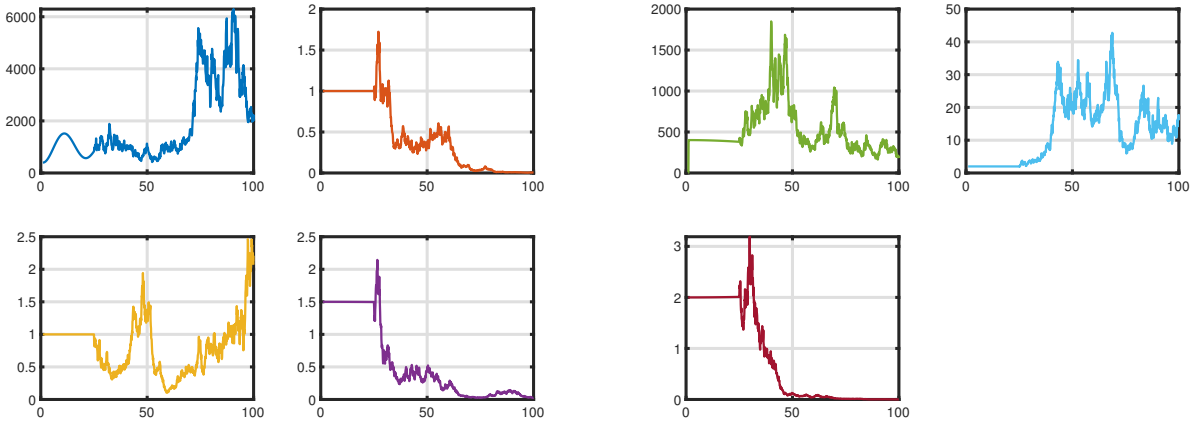

(a) **(b)**

Figure 10. The HIV-1/HTLV-I model exhibits deterministic-stochastic behaviour with humoral immune response and cellular outbreak (3.12)–(3.14) via the generalized Mittag-Leffler kernel with $\eta = 0.95$ and white noses with ICs $(400, 1, 1, 1.5, 4, 2, 2)$.

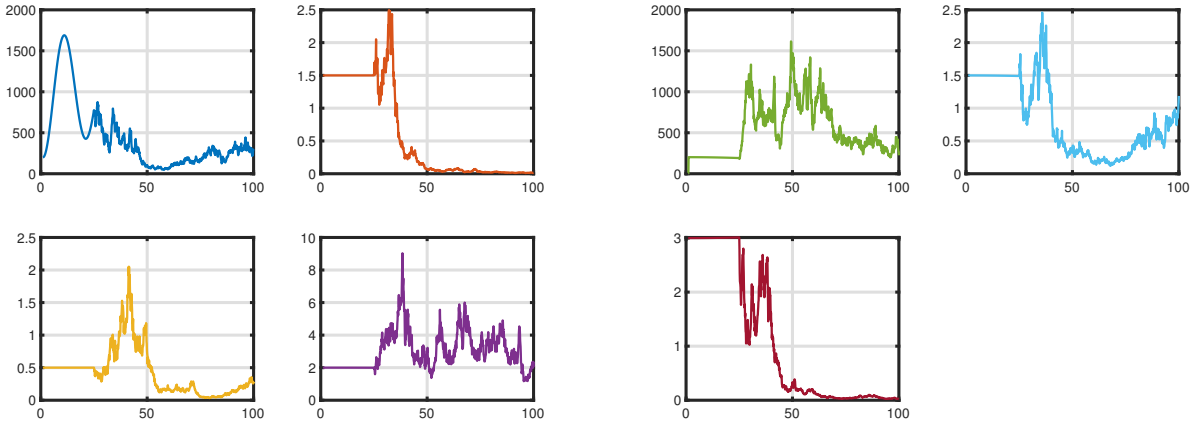

(a) **(b)**

Figure 11. The HIV-1/HTLV-I model exhibits deterministic-stochastic behaviour with humoral immune response and cellular outbreak (3.12)–(3.14) via the generalized Mittag-Leffler kernel with $\eta = 0.95$ and white noises with ICs of $(200, 1.5, 0.5, 2, 6, 1.5, 3)$.

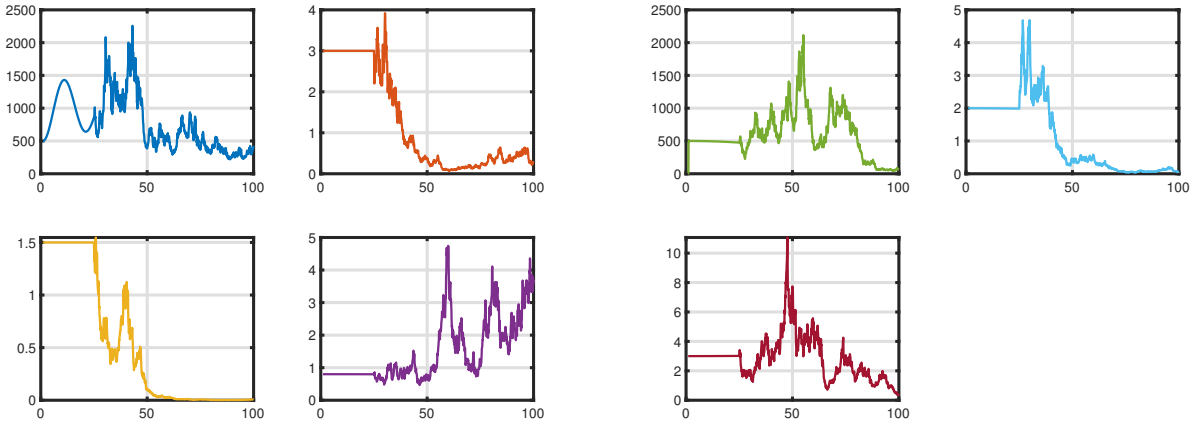

(a) **(b)**

Figure 12. The HIV-1/HTLV-I model exhibits deterministic-stochastic behaviour with humoral immune response and cellular outbreak (3.12)–(3.14) via the generalized Mittag-Leffler kernel with $\eta = 0.95$ and white noises with ICs of $(500, 3, 1.5, 0.8, 3, 2, 3)$.

Consider the biological parameters of the system (2.3), which supports the combination $(\mathcal{A}_5)$. Figure 13 depicts the implementation of the control and without control by considering the deterministic version of the system (2.1). The plots evidently depict the current work's goal. When δ increases, the intensities of HIV-1 particulate and latent/active HIV-1-infected CD4$^+$ T cells decrease, while the densities of latent/active HTLV-I-infected CD4$^+$ T cells increase. As a result, while HIV-1-specific immune responses can regulate HIV-1 infection, they may also accelerate the evolution of HTLV-I.

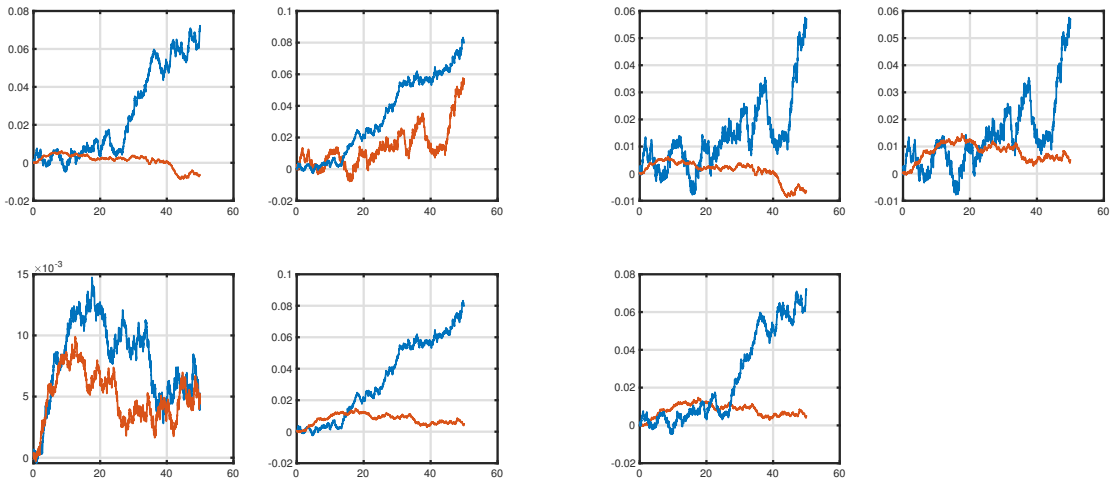

(a) **(b)**

Figure 13. Graphical illustration of the dynamical behavior of HIV-1/HTLV-I model with humoral immune response and cellular outbreak derived from model (2.3) in the presence (red-dotted zigzag) and absence (blue-dotted zigzag) of the control.

To investigate the local appropriate result of the HIV-1/HTLV-I model (2.1) for the true density function of the distribution, $\mathbb{T} = 2000$ is the total iteration time with condition $(\mathcal{A}_6)$. The frequency histograms of the HIV-1/HTLV-I model (2.1) are shown in Figure 14, along with the corresponding frequency histogram fitting curves of the system (2.1). The probability density function and histogram all nearly coincide with the corresponding fitting curves, implying that the fitting effect of the HIV-1/HTLV-I model (2.1) is not only local but also global.

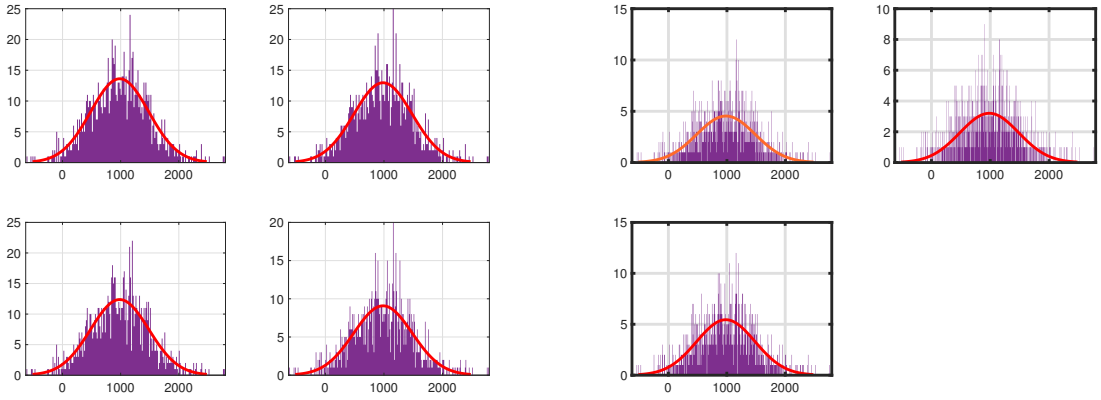

Figure 14. The seven histograms of the HIV-1/HTLV-I model with probability distribution and probability density functions for $(\mathcal{V}, \mathcal{G}^L, \mathcal{G}^A, \mathcal{U}^L, \mathcal{U}^A, \mathcal{T}, \mathcal{Q})$ are presented. The combination $(\mathcal{A}_6)$ determines the other specifications.

4. Conclusions

With the increasing occurrence and re-emergence of numerous disease outbreaks, self-preservation has emerged as a significant problem all over the world. We investigated a within-host HIV-1/HTLV-I codynamics system involving immune activation and both virus-to-cell and cell-to-cell mechanisms of propagation utilizing random perturbations and piecewise fractional differential operators. We describe our initial findings on the non-negativity and boundedness of the system's solutions. Furthermore, the presence of a stationary distribution in the system (2.3) was quantitatively authenticated by employing the Khasminskii concept and an appropriate Lyapunov formulation. According to threshold parameter $\mathbb{R}_0^p$, we determined the disease's extinction.

Besides that, we outlined the threshold parameter

$$\mathbb{R}_0^s = \frac{\upsilon_2\lambda(1-\lambda)}{(\beta+\frac{\wp_1^2}{2})(\epsilon+\xi+\frac{\wp_2^2}{2})(\varrho+\frac{\wp_3^2}{2})(\rho+\frac{\wp_6^2}{2})(\varkappa+\frac{\wp_7^2}{2})} > 1$$

for the unique ergodic and stationary distribution supported by Lyapunov functions. More specifically, it has been demonstrated that the vigour and authenticity of our simulated predictions and numerical results have been furnished with a piecewise fractional differential. Whereas the generalized Mittag-Leffler kernel, exponential decay and power law are currently shown to be effective in capturing multiple interconnection practises, we claim that the capacity to do so could potentially be confined by the enormity of biological form. We may infer that fluctuation may eradicate widespread signals while allowing transmittable illnesses to endure.

Several intriguing and unresolved issues merit additional deliberation. While analyzing the dynamic behavior of this type of challenge, it is necessary to investigate processes that are influenced by other considerations, including global stochastic Hopf bifurcations or oscillation frequency interference. In research just like this, a few accurate but intricate notions, such as assessing the impact of Markov transitions or Lévy and telegraph noise, can be involved. Such relevant aspects may indeed be addressed in the forthcoming analysis.

Use of AI tools declaration

The authors declare they have not used Artificial Intelligence (AI) tools in the creation of this article.

Conflict of interest

The authors declare no competing interests.

References

1. World Health Organization (WHO), HIV and AIDS, 2023. Available from: `http://www.who.int/mediacentre/factsheets/fs360/en/`.
2. H. Sato, J. Orensteint, D. Dimitrov, M. Martin, Cell-to-cell spread of HIV-1 occurs within minutes and may not involve the participation of virus particles, *Virology*, **186** (1992), 712–724. https://doi.org/10.1016/0042-6822(92)90038-q

3. D. S. Dimitrov, R. L. Willey, H. Sato, L. J. Chang, R. Blumenthal, M. A. Martin, Quantitation of human immunodeficiency virus type 1 infection kinetics, *J. Virol.*, **67** (1993), 2182–2190. https://doi.org/10.1128/jvi.67.4.2182-2190.1993
4. A. Sigal, J. T. Kim, A. B. Balazs, E. Dekel, A. Mayo, R. Milo, et al., Cell-to-cell spread of HIV permits ongoing replication despite antiretroviral therapy, *Nature*, **477** (2011), 95–98. https://doi.org/10.1038/nature10347
5. C. R. M. Bangham, The immune control and cell-to-cell spread of human T-lymphotropic virus type 1, *J. Gen. Virol.*, **84** (2003), 3177–3189. https://doi.org/10.1099/vir.0.19334-0
6. C. R. M. Bangham, The immune response to HTLV-I, *Curr. Opin. Immunol.*, **12** (2000), 397–402. https://doi.org/10.1016/s0952-7915(00)00107-2
7. P. Wu, H. Zhao, Dynamics of an HIV infection model with two infection routes and evolutionary competition between two viral strains, *Appl. Math. Model.*, **84** (2020), 240–264. https://doi.org/10.1016/j.apm.2020.03.040
8. P. Wu, S. Zheng, Z. He, Evolution dynamics of a time-delayed reactiondiffusion HIV latent infection model with two strains and periodic therapies, *Nonlinear Anal.-Real*, **67** (2022), 103559. https://doi.org/10.1016/j.nonrwa.2022.103559
9. P. Wu, H. Zhao, Dynamical analysis of a nonlocal delayed and diffusive HIV latent infection model with spatial heterogeneity, *J. Franklin. I.*, **358** (2021), 5552–5587. https://doi.org/10.1016/j.jfranklin.2021.05.014
10. C. Casoli, E. Pilotti, U. Bertazzoni, Molecular and cellular interactions of HIV-1/HTLV coinfection and impact on AIDS progression, *AIDS Rev.*, **9** (2007), 140–149.
11. M. T. Silva, O. de Melo Espíndola, A. C. C. B. Leite, A. Araújo, Neurological aspects of HIV/human T lymphotropic virus coinfection, *AIDS Rev.*, **11** (2009), 71–78.
12. C. Isache, M. Sands, N. Guzman, D. Figueroa, HTLV-1 and HIV-1 co-infection: A case report and review of the literature, *IDCases*, **4** (2016), 53–55. https://doi.org/10.1016/j.idcr.2016.03.002
13. M. A. Nowak, C. R. M. Bangham. Population dynamics of immune responses to persistent viruses, *Science*, **272** (1996), 74–79. https://doi.org/10.1126/science.272.5258.74
14. C. Mondal, D. Adak, N. Bairagi, Optimal control in a multi-pathways HIV-1 infection model: A comparison between mono-drug and multi-drug therapies, *Int. J. Control*, **94** (2021), 2047–2064. https://doi.org/10.1080/00207179.2019.1690694
15. X. Lai, X. Zou, Modeling HIV-1 virus dynamics with both virus-to-cell infection and cell-to-cell transmission, *SIAM J. Appl. Math.*, **74** (2014), 898–917. https://doi.org/10.1137/130930145
16. X. Wang, S. Tang, X. Song, L. Rong, Mathematical analysis of an HIV latent infection model including both virus-to-cell infection and cell-to-cell transmission, *J. Biol. Dyn.*, **11** (2016), 455–483. https://doi.org/10.1080/17513758.2016.1242784
17. A. M. Elaiw, N. H. AlShamrani, Stability of a general CTL-mediated immunity HIV infection model with silent infected cell-to-cell spread, *Adv. Differ. Equ.*, **2020** (2020), 355. https://doi.org/10.1186/s13662-020-02818-3
18. X. Ren, Y. Tian, L. Liu, X. Liu, A reaction–diffusion within-host HIV model with cell-to-cell transmission, *J. Math. Biol.*, **76** (2018), 1831–1872. https://doi.org/10.1007/s00285-017-1202-x

19. W. Wang, X. Wang, K. Guo, W. Ma, Global analysis of a diffusive viral model with cell-to-cell infection and incubation period, *Math. Method. Appl. Sci.*, **43** (2020), 5963–5978. https://doi.org/10.1002/mma.6339
20. N. H. AlShamrani, M. A. Alshaikh, A. M. Elaiw, K. Hattaf, Dynamics of HIV-1/HTLV-I co-infection model with humoral immunity and cellular infection, *Viruses*, **14** (2022), 1719. https://doi.org/10.3390/v14081719
21. A. Atangana, Extension of rate of change concept: From local to nonlocal operators with applications, *Results Phys.*, **19** (2021), 103515. https://doi.org/10.1016/j.rinp.2020.1
22. A. Atangana, J. F. Gomez-Aguilar, Fractional derivatives with no-index law property: Application to chaos and statistics, *Chaos Soliton. Fract.*, **114** (2018), 516–535. https://doi.org/10.1016/j.chaos.2018.07.033
23. F. Jarad, T. Abdeljawad, Z. Hammouch, On a class of ordinary differential equations in the frame of Atangana–Baleanu fractional derivative, *Chaos Soliton. Fract.*, **117** (2018), 16–20. https://doi.org/10.1016/j.chaos.2018.10.006
24. M. Caputo, Linear models of dissipation whose Q is almost frequency independent-II, *Geophys. J. Int.*, **13** (1967), 529–539. https://doi.org/10.1111/j.1365-246X.1967.tb02303.x
25. M. Caputo, M. Fabrizio, A new definition of fractional derivative without singular kernel, *Progr. Fract. Differ. Appl.*, **1** (2015), 73–85.
26. A. Atangana, D. Baleanu, New fractional derivatives with non-local and non-singular kernel: Theory and application to heat transfer model, *Thermal Sci.*, **20** (2016), 763–769. https://doi.org/10.2298/TSCI160111018A
27. T. Abdeljawad, Q. M. Al-Mdallal, Discrete Mittag-Leffler kernel type fractional difference initial value problems and Gronwall's inequality, *J. Comput. Appl. Math.*, **339** (2018), 218–230. https://doi.org/10.1016/j.cam.2017.10.021
28. A. Kumar, S. Kumar, A study on eco-epidemiological model with fractional operators, *Chaos Soliton. Fract.*, **156** (2022), 111697. https://doi.org/10.1016/j.chaos.2021.111697
29. B. Ghanbari, S. Kumar, R. Kumar, A study of behaviour for immune and tumor cells in immunogenetic tumour model with non-singular fractional derivative, *Chaos Solit. Fract.*, **133** (2020), 109619. https://doi.org/10.1016/j.chaos.2020.109619
30. A. Atangana, S. I. Araz, New concept in calculus: Piecewise differential and integral operators, *Chaos Soliton. Fract.*, **145** (2021), 110638. https://doi.org/10.1016/j.chaos.2020.110638
31. A. Atangana, S. I. Araz, Deterministic-stochastic modeling: A new direction in modeling real world problems with crossover effect, *Math. Biosci. Eng.*, **19** (2022), 3526–3563. https://doi.org/10.3934/mbe.2022163
32. M. A. Qurashi, S. Rashid, F. Jarad, A computational study of a stochastic fractal-fractional hepatitis B virus infection incorporating delayed immune reactions via the exponential decay, *Math. Biosci. Eng.*, **19** (2022), 12950–12980. https://doi.org/10.3934/mbe.2022605
33. S. Rashid, M. K. Iqbal, A. M. Alshehri, R. Ashraf, F. Jarad, A comprehensive analysis of the stochastic fractal-fractional tuberculosis model via Mittag-Leffler kernel and white noise, *Results Phys.*, **39** (2022), 105764. https://doi.org/10.1016/j.rinp.2022.105764

34. A. M. Elaiw, N. H. AlShamrani, Modeling and analysis of a within-host HIV/HTLV-I co-infection, *Bol. Soc. Mat. Mex.*, **27** (2021), 38. https://doi.org/10.1007/s40590-021-00330-6

35. B. Zhou, D. Jiang, Y. Dai, T. Hayat, Threshold dynamics and probability density function of a stochastic avian influenza epidemic model with nonlinear incidence rate and psychological effect, *J. Nonlinear Sci.*, **33** (2023), 29. https://doi.org/10.1007/s00332-022-09885-8

36. Y. M. Chu, S. Sultana, S. Rashid, M. S. Alharthi, Dynamical analysis of the stochastic COVID-19 model using piecewise differential equation technique, *Comput. Model. Eng. Sci.*, **137** (2023), 2427–2464. https://doi.org/10.32604/cmes.2023.028771

37. S. Rashid, F. Jarad, S. A. A. El-Marouf, S. K. Elagan, Global dynamics of deterministic-stochastic dengue infection model including multi specific receptors via crossover effects, *AIMS Mathematics*, **8** (2022), 6466–6503. https://doi.org/10.3934/math.2023327

38. A. S. Perelson, D. E. Kirschner, R. De Boer, Dynamics of HIV infection of $CD4^+$ T cells, *Math. Biosci.*, **114** (1993), 81–125. https://doi.org/10.1016/0025-5564(93)90043-a

39. D. S. D. S. Callaway, A. S. Perelson, HIV-1 infection and low steady state viral loads, *Bull. Math. Biol.*, **64** (2002), 29–64. https://doi.org/10.1006/bulm.2001.0266

40. H. Mohri, S. Bonhoeffer, S. Monard, A. S. Perelson, D. D. Ho, Rapid turnover of T lymphocytes in SIV-infected rhesus macaques, *Science*, **279** (1998), 1223–1227. https://doi.org/10.1126/science.279.5354.1223

41. Y. Wang, J. Liu, L. Liu, Viral dynamics of an HIV model with latent infection incorporating antiretroviral therapy, *Adv. Differ. Equ.*, **2016** (2016), 225. https://doi.org/10.1186/s13662-016-0952-x

42. A. S. Perelson, A. U. Neumann, M. Markowitz, J. M. Leonard, D. D. Ho, HIV-1 dynamics in vivo: Virion clearance rate, infected cell life-span, and viral generation time, *Science*, **271** (1996), 1582–1586. https://doi.org/10.1126/science.271.5255.1582

43. P. W. Nelson, J. D. Murray, A. S. Perelson, A model of HIV-1 pathogenesis that includes an intracellular delay, *Math. Biosci.*, **163** (2000), 201–215. https://doi.org/10.1016/s0025-5564(99)00055-3

44. A. S. Perelson, P. W. Nelson, Mathematical analysis of HIV-1 dynamics in vivo, *SIAM Rev.*, **41** (1999), 3–44. https://doi.org/10.1137/S0036144598335107

45. M. Y. Li, A. G. Lim, Modelling the role of Tax expression in HTLV-1 persisence in vivo, *Bull. Math. Biol.*, **73** (2011), 3008–3029. https://doi.org/10.1007/s11538-011-9657-1

46. Y. Wang, J. Liu, J. M. Heffernan, Viral dynamics of an HTLV-I infection model with intracellular delay and CTL immune response delay, *J. Math. Anal. Appl.*, **459** (2018), 506–527. https://doi.org/10.1016/j.jmaa.2017.10.027

47. L. Wang, Z. Liu, Y. Li, D. Xu, Complete dynamical analysis for a nonlinear HTLV-I infection model with distributed delay, CTL response and immune impairment, *Discret Cont. Dyn.-B*, **25** (2020), 917–933. https://doi.org/10.3934/dcdsb.2019196

48. A. M. Elaiw, A. A. Raezah, A. S. Alofi, Effect of humoral immunity on HIV-1 dynamics with virus-to-target and infected-to-target infections, *AIP Adv.*, **6** (2016), 085204. https://doi.org/10.1063/1.4960987

49. L. Imhof, S. Walcher, Exclusion and persistence in deterministic and stochastic chemostat models, *J. Differ. Equ.*, **217** (2005), 26–53. https://doi.org/10.1016/j.jde.2005.06.017

50. X. Mao, *Stochastic differential equations and applications*, Chichester: Horwood Publishing, 1997.

51. R. Khasminskii, *Stochastic stability of differential equations*, Heidelberg, Berlin: Springer, 2012. https://doi.org/10.1007/978-3-642-23280-0

52. R. S. Lipster, A strong law of large numbers for local martingales, *Stochastics*, **3** (1980), 217–228. https://doi.org/10.1080/17442508008833146

AIMS Press